J|A|C|S
ARTICLES

Published on Web 11/01/2008

Cationic Terminal Gallylene Complexes by Halide Abstraction: Coordination Chemistry of a Valence Isoelectronic Analogue of CO and N_2

Natalie D. Coombs,[†,‡] Dragoslav Vidovic,[†] Joanna K. Day,[†,‡] Amber L. Thompson,[†] Delphine D. Le Pevelen,[†] Andreas Stasch,[§] William Clegg,[||] Luca Russo,[||] Louise Male,[⊥] Michael B. Hursthouse,[⊥] David J. Willock,[‡] and Simon Aldridge*[,†]

Inorganic Chemistry, University of Oxford, South Parks Road, Oxford, U.K. OX1 3QR, Cardiff School of Chemistry, Main Building, Park Place, Cardiff, U.K. CF10 3AT, School of Chemistry, Monash University, P.O. Box 23, Victoria 3800, Australia, School of Chemistry, Bedson Building, Newcastle University, Newcastle upon Tyne, U.K. NE1 7RU, and School of Chemistry, University of Southampton, Southampton, U.K. SO17 1BJ

Received August 22, 2008; E-mail: Simon.Aldridge@chem.ox.ac.uk

Abstract: While N_2 and CO have played central roles in developing models of electronic structure, and their interactions with transition metals have been widely investigated, the valence isoelectronic diatomic molecules EX (E = group 13 element, X = group 17 element) have yet to be isolated under ambient conditions, either as the "free" molecule or as a ligand in a simple metal complex. As part of a program designed to address this deficiency, together with wider issues of the chemistry of cationic systems $[L_nM(ER)]^+$ (E = B, Al, Ga; R = aryl, amido, halide), we have targeted complexes of the type $[L_nM(GaX)]^+$. Halide abstraction is shown to be a viable method for the generation of mononuclear cationic complexes containing gallium donor ligands. The ability to isolate tractable two-coordinate products, however, is strongly dependent on the steric and electronic properties of the metal/ligand fragment. In the case of complexes containing ancillary π-acceptor ligands such as CO, cationic complexes can only be isolated as base-trapped adducts, even with bulky aryl substituents at gallium. *Base-free* gallylene species such as $[Cp^*Fe(CO)_2(GaMes)]^+$ can be identified only in the vapor phase by electrospray mass spectrometry experiments. With bis(phosphine) donor sets at the metal, the more favorable steric/electronic environment allows for the isolation of two-coordinate ligand systems, *even with halide substituents at gallium*. Thus, $[Cp^*Fe(dppe)(GaI)]^+[BAr^f_4]^-$ (**9**) can be synthesized and shown crystallographically to feature a terminally bound GaI ligand; **9** represents the first experimental realization of a complex containing a valence isoelectronic group 13/group 17 analogue of CO and N_2. DFT calculations reveal a relatively weakly bound GaI ligand, which is confirmed experimentally by the reaction of **9** with CO to give $[Cp^*Fe(dppe)(CO)]^+[BAr^f_4]^-$. In the absence of such reagents, **9** is stable for weeks in fluorobenzene solution, presumably reflecting (i) effective steric shielding of the gallium center by the ancillary phosphine and Cp* ligands; (ii) a net cationic charge which retards the tendency toward dimerization found for putative charge neutral systems; and (iii) (albeit relatively minor) population of the LUMOs of the GaI molecule through π overlap with the HOMO and HOMO-2 of the $[Cp^*Fe(dppe)]^+$ fragment.

Introduction

The fundamental changes in electronic structure which accompany the interaction of a diatomic molecule with a transition metal center have been exploited to great effect in coordination chemistry,[1] both in the activation of inherently inert molecules (such as N_2)[2] and in the isolation and characterization of otherwise labile species (e.g., CX, where X = S, Se, Te).[3] Thus, for example, relevance to the biological conversion of N_2 to NH_3 was the driving force behind the isolation of the first dinitrogen complexes in 1965;[4] by contrast, the stronger metal−ligand bonds formed by the isoelectronic CO molecule underpin its widespread exploitation in low oxidation state transition metal chemistry (ca. 35,000 structurally characterized examples).[5] Within this family of ten valence electron diatomic molecules, species of the type EX (E = group 13 element, X = group 17 element), although predicted to be inherently less stable in the "free" state (due to small HOMO/LUMO gaps),

[†] University of Oxford.
[‡] Cardiff School of Chemistry.
[§] Monash University.
[||] Newcastle University.
[⊥] University of Southampton.

(1) See, for example: (a) Thorp, H. H. *Science* **2000**, *289*, 882.
(2) Laplaza, C. E.; Cummins, C. C. *Science* **1995**, *268*, 861.
(3) (a) Baird, M. C.; Wilkinson, G. *Chem. Commun. (London)* **1966**, 267. (b) Clark, G. R.; James, S. M. *J. Organomet. Chem.* **1977**, *134*, 229. (c) Clark, G. R.; Marsden, K.; Roper, W. R.; Wright, L. J. *J. Am. Chem. Soc.* **1980**, *102*, 1206. (d) Clark, G. R.; Marsden, K.; Rickard, C. E. F.; Roper, W. R.; Wright, L. J. *J. Organomet. Chem.* **1988**, *338*, 393.
(4) Allen, A. D.; Senoff, C. V. *Chem. Commun. (London)* **1965**, 621.
(5) As determined from a survey of the Cambridge Structural Database 22/08/2008.

are thought to offer *even more favorable* thermodynamics of binding to metal centers.[6−8] Such predictions stem from the stronger σ donor properties (higher HOMO energies) expected for group 13 donor ligands and the greater amplitude of the π acceptor LUMO at E. Despite this, the complexes so formed $[L_nM(EX)]$ are also expected to be extremely labile, due to the buildup of positive charge at the group 13 element, E.[6−8] Superficially, this reflects not only the inherent disparity in electronegativities between group 13 and group 17 elements[9]but also the removal of further electron density from E on coordination to a transition metal. With this in mind, and given the relative electronegativities of the group 17 elements, iodine perhaps represents the optimal choice of halogen substituent, X.

From a synthetic perspective, a further obstacle is the lack of readily available sources of the diatomic EX molecule. Thus, while N_2 and CO are stable diatomic gases and their introduction into metal coordination spheres has been achieved by a variety of methods,[10] BX (X = F, Cl), AlX (X = F, Cl, Br, I), and GaX (X = Cl, Br, I) are known (as donor-free species) only under conditions of extreme temperature, with problems stemming from disproportionation or aggregation inherent at (or close to) room temperature.[7a,11−14] Synthetic methodologies based on coordination of the "free" EX molecule therefore seem likely to flounder, and we have sought to exploit an alternative methodology, that is abstraction of a halide anion (X^-) from a pre-existing metal complex of the type $L_nM(EX_2)$.[15−19] Such an approach necessarily generates a cationic complex of the type $[L_nM(EX)]^+$, thereby imposing an electrostatic barrier to oligomerization processes such as those thought to be important for charge-neutral analogues such as $[(\eta^5\text{-}C_5H_4Me)Mn(CO)_2BCl]$.[7b] That said, such cationic derivatives are also likely to be highly electrophilic, and the steric/electronic properties of peripheral substituents will therefore play key roles in determining thermodynamic stability and/or kinetic lability. Thus, for example, in the case of borylene complexes $[L_nM(BR)]^+$, electronic structure has been shown to be strongly dependent on the π-donor properties of the boron-bound substituent, e.g. Fischer carbene-like M=B double bonds for B(σ-aryl), simple M ← B donor/acceptor interactions for B(η^5-Cp*), and intermediate behavior for $B(NR_2)$.[15a,e,17] However, if simple halogen-substituted derivatives, $[L_nM(EX)]^+$, are sought, opportunities for variation in sterics/electronics lie primarily with the metal/ligand fragment. We have therefore targeted bulky, electron-rich systems L_nM, which are known to bind the diatomics CO and N_2 (e.g., $[(\eta^5\text{-}C_5R_5)M(PR_3)_2]^+$, where M = a group 8 metal)[20] and which are likely to offer both steric and electronic protection of the coordinated EX ligand.[21] By utilizing this approach, we have been able to target cationic compounds containing gallylene ligands $\{[L_nM(GaR)]^+$; R = aryl, amido, halide$\}$, including the successful isolation of $[Cp^*Fe(dppe)(GaI)]^+[BAr^f_4]^-$ [Ar^f = $C_6H_3(CF_3)_2$-3,5]. This complex features a terminally bound GaI ligand and, therefore, represents the first experimental realization of a valence isoelectronic group 13/group 17 analogue of CO and N_2.[16] Given the heated debate concerning models of metal−metal bonding in gallium-containing systems[22] and, for example, the description of superficially similar complexes as being bound via multiple bonds (e.g., $L_nM{\equiv}ER$) or via donor/acceptor interactions ($L_nM \leftarrow ER$),[23] we perceived such complexes as ideal platforms on which to test bonding models by quantum chemical methods. In addition, we have also sought to compare ligand properties with related ten valence electron systems such as N_2, CO, and BF.

Experimental Section

(i) General Considerations. All manipulations were carried out under a nitrogen or argon atmosphere using standard Schlenk line

(6) (a) Ehlers, A. W.; Baerends, E. J.; Bickelhaupt, F. M.; Radius, U. *Chem.—Eur. J.* **1998**, *4*, 210. (b) Radius, U.; Bickelhaupt, F. M.; Ehlers, A. W.; Goldberg, N.; Hoffmann, R. *Inorg. Chem.* **1998**, *37*, 1080. (c) Frenking, G.; Fröhlich, N. *Chem. Rev.* **2000**, *100*, 717.

(7) Complexes containing a terminally bound EX ligand have been postulated as labile intermediates. See, for example: (a) Timms, P. L. *Acc. Chem. Res.* **1973**, *6*, 118. (b) Braunschweig, H.; Colling, M.; Hu, C.; Radacki, K. *Angew. Chem., Int. Ed.* **2002**, *41*, 1359.

(8) Examples of *three-coordinate* bridging EX ligands simultaneously bonded to two metal centers are known. See, for example: (a) Bunn, N. R.; Aldridge, S.; Kays (née Coombs) , D. L.; Coombs, N. D.; Day, J. K.; Ooi, L.-L.; Coles, S. J.; Hursthouse, M. B. *Organometallics* **2005**, *24*, 5879. (b) Bissinger, P.; Braunschweig, H.; Seeler, F. *Organometallics* **2007**, *26*, 4700.

(9) Emsley, J. *The Elements*; Oxford University Press: Oxford, 1991.

(10) See, for example: (a) Collman, J. P.; Hegedus, L. S.; Norton, J. R.; Finke, R. G. *Principles and Applications of Organotransition Metal Chemistry*; University Science Books: Sausalito, CA, 1987.

(11) (a) Timms, P. L. *J. Am. Chem. Soc.* **1967**, *89*, 1629. (b) Timms, P. L. *J. Am. Chem. Soc.* **1968**, *90*, 4585.

(12) (a) Dohmeier, C.; Loos, D.; Schnöckel, H. *Angew. Chem., Int. Ed.* **1996**, *35*, 129. (b) Schnepf, A.; Schnöckel, H. *Angew. Chem., Int. Ed.* **2002**, *41*, 3532. (c) Koch, K.; Burgert, R.; Schnöckel, H. *Angew. Chem., Int. Ed.* **2007**, *46*, 5795.

(13) With regard to gallium(I) iodide, the phosphine donor-stabilized cluster $Ga_8I_8(PEt_3)_6$ has been reported: (a) Doriat, C.; Friesen, M.; Baum, E.; Ecker, A.; Schnöckel, H. *Angew. Chem., Int. Ed. Engl.* **1997**, *36*, 1969. In addition, a sparingly soluble reagent of uncertain composition formulated as "GaI" has also been described. (b) Green, M. L. H.; Mountford, P.; Smout, G. J.; Speel, S. R. *Polyhedron* **1990**, *9*, 2763. (c) Baker, R. J.; Jones, C. *Dalton Trans.* **2005**, 1341.

(14) For a recent review encompassing aspects of group 13 sub-halides isolated in inert gas matrices, see, for example:(a) Himmel, H.-J. *Z. Anorg. Allg. Chem.* **2005**, *631*, 1551, and references therein.

(15) See, for example: (a) Coombs, D. L.; Aldridge, S.; Jones, C.; Willock, D. J. *J. Am. Chem. Soc.* **2003**, *125*, 6356. (b) Bunn, N. R.; Aldridge, S.; Coombs, D. L.; Rossin, A.; Willock, D. J.; Jones, C.; Ooi, L.-L. *Chem. Commun.* **2004**, 1732. (c) Kays, D. L.; Aldridge, S.; Day, J. K.; Ooi, L.-L. *Angew. Chem., Int. Ed.* **2005**, *44*, 7457. (d) Bunn, N. R.; Aldridge, S.; Kays, D. L.; Coombs, N. D.; Rossin, A.; Willock, D. J.; Jones, C.; Ooi, L.-L. *Organometallics* **2005**, *24*, 5891. (e) Aldridge, S.; Jones, C.; Gans-Eichler, T.; Stasch, A.; Kays (née Coombs) , D. L.; Coombs, N. D.; Willock, D. J. *Angew. Chem., Int. Ed* **2006**, *45*, 6118.

(16) For a preliminary account of part of this work, see: (a) Coombs, N. D.; Clegg, W.; Thompson, A. L.; Willock, D. J.; Aldridge, S. *J. Am. Chem. Soc.* **2008**, *130*, 5449. (b) Himmel, H.-J.; Linti, G. *Angew. Chem., Int. Ed.* **2008**, *47*, 6326 (highlight article)

(17) (a) Braunschweig, H.; Radacki, K.; Uttinger, K. *Angew. Chem., Int. Ed.* **2007**, *46*, 3979. (b) Braunschweig, H.; Kraft, K.; Kupfer, F.; Radacki, K.; Seeler, F. *Angew. Chem., Int. Ed.* **2008**, *47*, 4931.

(18) Vidovic, D.; Findlater, M.; Reeske, G.; Cowley, A. H. *Chem. Commun.* **2006**, 3786.

(19) For a related approach utilizing protonation of a gallium-bound hydrocarbyl substituent to generate a cationic complex, see: (a) Cadenbach, T.; Gemel, C.; Zacher, D.; Fischer, R. A. *Angew. Chem., Int. Ed.* **2008**, *120*, 3487.

(20) See, for example:(a) Glaser, P. B.; Wanandi, P. W.; Tilley, T. D. *Organometallics* **2004**, *23*, 693. (b) Paul, F.; Toupet, L.; Roisnel, T.; Hamon, P.; Lapinte, C. C. R. *Chimie* **2005**, *8*, 1174.

(21) (a) Ueno, K.; Watanabe, T.; Tobita, H.; Ogino, H. *Organometallics* **2003**, *22*, 4375. (b) Muraoka, T.; Motohashi, H.; Hirotsu, M.; Ueno, K. *Organometallics* **2008**, *27*, 3918.

(22) See, for example: (a) Su, J.; Li, X.-W.; Crittendon, R. C.; Campana, C. F.; Robinson, G. H. *Organometallics* **1997**, *16*, 4511. (b) Cotton, F. A.; Feng, X. *Organometallics* **1998**, *17*, 128.

(23) For recent reviews of the coordination chemistry of diyl ligands, see, for example: (a) Fischer, R. A.; Weiβ, J. *Angew. Chem., Int. Ed.* **1999**, *38*, 2830. (b) Linti, G.; Schnöckel, H. *Coord. Chem. Rev.* **2000**, *206−207*, 285. (c) Cowley, A. H. *Chem. Commun.* **2004**, 2369. (d) Gemel, C.; Steinke, T.; Cokoja, M.; Kempter, A.; Fischer, R. A. *Eur. J. Inorg. Chem.* **2004**, 4161. (e) Aldridge, S.; Coombs, D. L. *Coord. Chem. Rev.* **2004**, *248*, 535. (f) Braunschweig, H.; Rais, D.; Kollann, C. *Angew. Chem., Int. Ed.* **2006**, *45*, 5254.

(24) Barry, S. T.; Richeson, D. S. *Chem. Mater.* **1994**, *6*, 2220.

or drybox techniques. Solvents were predried over sodium wire (hexanes, toluene, diethyl ether) or molecular sieves (dichloromethane, fluorobenzene) and purged with nitrogen prior to distillation from the appropriate drying agent (hexanes, potassium; toluene or diethyl ether, sodium; dichloromethane or fluorobenzene, CaH_2). d_6-Benzene, d_2-dichloromethane, and d_5-fluorobenzene (all Goss) were degassed and dried over the appropriate drying agent (potassium or molecular sieves) prior to use. MesLi (Mes = 2,4,6-$Me_3C_6H_2$), $(Me_3Si)_2NGaCl_2 \cdot THF$,[24] $Na[BAr^f_4]$ [Ar^f = $C_6H_3(CF_3)_2$-3,5],[25] $Na[(\eta^5\text{-}C_5R_5)Fe(CO)_2]$ (R = H, Me),[26] and $[Cp^*Fe(CO)_2GaI_2]_2$ (**1**)[8a] were synthesized by literature routes; the synthetic procedure for $[Cp^*Ru(CO)_2GaI_2]_2$ (**13**) and details of its reactivity toward dppe are included in the Supporting Information. Reagents dppe, carbon monoxide, 4,4′-di-*tert*-butyl-2,2′-bipyridyl (dtbpy) and [^{n}Bu$_4$N]I were used as received.

NMR spectra were measured on Bruker AM-400, Jeol 300 Eclipse Plus, or Varian Mercury 300 FT-NMR spectrometers. Residual signals of solvent were used for reference for ^{1}H and ^{13}C NMR spectroscopy. ^{11}B, ^{19}F, and ^{31}P NMR spectra were referenced with respect to $Et_2O \cdot BF_3$, $CFCl_3$, and 85% aqueous H_3PO_4, respectively. Infrared spectra were measured for each compound either pressed into a disk with excess dry KBr or as a solution in the appropriate solvent, on a Nicolet 500 FT-IR spectrometer. Mass spectra were measured on a Bruker MicroTOF-Q instrument with direct sampling from a Braun LabMaster inert atmosphere box at the University of Bath (compound **9**)[27] or by the EPSRC National Mass Spectrometry Service Center, at the University of Wales Swansea. Perfluorotributylamine was used as the standard for high-resolution EI mass spectra. Elemental microanalysis data is reported for all compounds, except in cases were either extreme air and moisture sensitivity or the presence of volatile solvent within the crystal lattice precluded reliable reproducible measurements. For these compounds (**2**, **4**, and **9**), characterization is therefore based upon multinuclear NMR, IR, and mass spectrometry data (including accurate mass measurement), supplemented by single crystal X-ray diffraction studies. In all cases, the purity of the bulk material was established by multinuclear NMR to be >95%. Photolytic experiments were carried out using a Spectral Energy mercury arc lamp (1 kW) with samples contained within quartz Schlenk vessels. Spectroscopic abbreviations: m = multiplet, s = singlet, d = doublet, t = triplet, sept = septet, st = strong.

(ii) Crystallographic Method. Low temperature single crystal X-ray diffraction data for compounds **2**−**5**, **7**, **10**, **13**−**15**, and **17** were collected on an Nonius KappaCCD diffractometer; those for **9** and **11** were collected at the Daresbury Synchrotron Radiation Source on station 9.8. For compounds **2**−**5**, **7**, **10**, **13**−**15**, and **17**, data collection and cell refinement were carried out using DENZO and COLLECT,[28a,b] while, for **9** and **11**, the Bruker APEX2 software (including SAINT) was used.[28c] Structure solution and refinement were carried out with the SHELX software suite[28c] for compounds **2** and **3** (solved using DIRDIF-99),[28d] together with **7**, **9**, **11**, and **13**; the remaining structures (**4**, **5**, **10**, **14**, **15**, and **17**) were solved with SIR-92,[28e] and refined using CRYSTALS.[28f] Intensity data were processed and corrected for absorption effects by the multiscan method, based on multiple scans of identical and Laue equivalent reflections using the appropriate software (DENZO,[28a] SADABS,[28c] or SORTAV[28g]). In general, coordinates and anisotropic displacement parameters of all non-hydrogen atoms were refined except where this was not possible due to the presence of disorder. In most cases, the hydrogen atoms were visible in the difference map, but in general, they were positioned geometrically (then optimized by refinement with restraints for compounds **4**, **5**, **10**, **14**, **15**, and **17**) and refined using a riding model. The structure of compound **13** (isomorphous with previously reported **1**)[8a] and those of **7**, **10**, **11**, **13**−**15**, and **17**, which were obtained merely for confirmation of composition, are included only in the Supporting Information. For the remaining compounds (**2**−**5** and **9**), the details of each data collection, structure solution, and refinement can be found in Table 1. Relevant bond lengths and angles are included in the figure captions, and complete details of each structure have been deposited with the CCDC (numbers as listed in Table 1). In addition, complete details for each structure (including CIF files) have been included in the Supporting Information. In the case of compound **9**, the structural model has the iodine atom disordered over three sites, with the two main sites being occupied in the ratio 3.8:1. The major site gives an almost linear Fe−Ga−I unit (ca. 171°), while the minor site is rather more bent (ca. 149°) and features contacts between I′ and C(55)−C(58) of one aromatic ring of the $[BAr^f_4]^-$ anion which are within the sum of the van der Waals radii for iodine and carbon. There is also a very small contribution (1.85%) of the neutral starting material, substituted on the cation site, with a corresponding slight deficiency on the anion site. Details of minor disorder in other structures are included in the Supporting Information.

(iii) Computational Method. The geometries of the model complexes $[CpFe(dmpe)(EX)]^+$ (EX = GaI, BF, CO, N_2) were optimized using ADF (BLYP/TZP) using widely precedented and previously described methods.[29] In order to investigate quantitatively the ability of the Fe−Ga−I unit in complex **9** to adopt nonlinear geometries, a series of further calculations was carried out using the B3LYP functional within the Gaussian03 package on a more realistic model system in which the dppe ligand was reduced to $Me(Ph)PCH_2CH_2P(Ph)Me$ with the Ph groups proximal to the GaI ligand being retained; the methyl groups of the Cp* ligand were also included in the calculation. Calculations of σ and π contributions to bonding densities were then carried out as reported previously for analogous investigations of transition metal diyl and boryl complexes.[29] To carry out the desired energy decomposition analyses, the fully optimized structure was split into two fragments: $[CpFe(dmpe)]^+$ and the EX ligand. For each fragment, molecular orbitals were calculated using a TZP basis set in the geometry of the complete complex and these were then used as the basis in a further SCF computation on the full structure. This approach allows ADF to give a breakdown of the interaction between $[CpFe(dmpe)]^+$ and each of the diatomic ligands. An alternative breakdown of the fragment interaction energy into contributions from the Hamiltonian potentials was also carried out (see Supporting Information).

(iv) Syntheses. Cp*Fe(dppe)GaI$_2$ (3). To a solution of $[Cp^*Fe(CO)_2GaI_2]_2$ (**1**; 1.414 g, 1.240 mmol) in toluene (100 cm^3) was added a solution of dppe (1.110 g, 2.785 mmol) also in toluene (200 cm^3), and the reaction mixture was photolyzed for 86 h. The resulting dark orange solution was filtered and concentrated in *vacuo*, and red crystals of **3** suitable for X-ray diffraction were obtained from a concentrated toluene solution at −30 °C. Isolated yield 0.789 g, 35%. ^{1}H NMR (C_6D_6, 300 MHz): δ_H 1.33 (s, 15H,

(25) Reger, D. L.; Wright, T. D.; Little, C. A.; Lamba, J. J. S.; Smith, M. D. *Inorg. Chem.* **2001**, *40*, 3810.
(26) (a) King, R. B.; Bisnette, M. B. *J. Organomet. Chem.* **1967**, *8*, 287. (b) King, R. B. *Acc. Chem. Res.* **1970**, *3*, 417.
(27) For a full description of the experimental approach used, see: (a) Lubben, A. T.; McIndoe, J. S.; Weller, A. S. *Organometallics* **2008**, *27*, 3303.
(28) (a) Denzo: Otwinowski, Z.; Minor, W. In *Methods Enzymology*; Carter, C. W., Sweet, R. M., Eds.; Academic Press: New York, 1996; Vol. 276, p 307. (b) Collect: Nonius B.V.: Delft, The Netherlands, 1997−1002. (c) Sheldrick, G. M. *Acta Crystallogr., Sect. A* **2008**, *64*, 112. (d) DIRDIF-99: Beurskens, P. T.; Admiraal, G.; Beurskens, G.; Bosman, W. P.; de Gelder, R.; Israel, R.; Smits, J. M. M. *The DIRDIF-99 Program System, Technical Report of the Crystallography Laboratory*; University of Nijmegen: Nijmegen, The Netherlands, 1999. (e) Sir-92: Altomare, A.; Cascarano, G.; Giacovazzo, C.; Guagliardi, A.; Burla, M. C.; Polidori, G.; Camalli, M. *J. Appl. Crystallogr.* **1994**, *27*, 435. (f) CRYSTALS: Betteridge, P. W.; Carruthers, J. R.; Cooper, R. I.; Prout, J.; Watkin, D. J. *J. Appl. Crystallogr.* **2003**, *36*, 1487. (g) Sortav: Blessing, R. H. *Acta Crystallogr., Sect. A* **1995**, *51*, 33.
(29) For previous DFT studies of related systems, see, for example: (a) Dickinson, A. A.; Willock, D. J.; Calder, R. J.; Aldridge, S. *Organometallics* **2002**, *21*, 1146. (b) Aldridge, S.; Rossin, A.; Coombs, D. L.; Willock, D. J. *Dalton Trans.* **2004**, 2649.

Table 1. Crystallographic Data for Compounds **2**−**5** and **9**

	2·(C_7H_8)	**3**·$^5/_4$(C_7H_8)	**4**·$^3/_4$(OC_4H_{10})	**5**	**9**
empirical formula	$C_{44}H_{47}FeGaI_2OP_2$	$C_{44.75}H_{49}Fe_1Ga_1I_2P_2$	$C_{45}H_{57.5}FeGaIO_{0.75}P_2$	$C_{21}H_{26}FeGaIO_2$	$C_{68}H_{51}BF_{24}FeGaIP_2$
CCDC deposition no.	699420	673696	699421	699422	673697
formula wt	1033.13	1028.15	960.90	562.91	1649.31
temp (K)	150(2)	150(2)	150(2)	150(2)	120(2)
wavelength (Å)	0.71073	0.71073	0.71073	0.71073	0.6710
cryst syst	monoclinic	triclinic	monoclinic	monoclinic	triclinic
space group	$P2_1/c$	$P\bar{1}$	$P12_1/c$	$P12_1/n$	$P\bar{1}$
unit cell lengths: a, b, c (Å)	11.068(2), 24.636(5), 15.587(3)	11.024(1), 19.064(1), 22.204(1)	14.531(1), 15.237(1), 21.020(1)	12.794(1), 12.896(1), 13.432(1)	12.582(1), 14.204(2), 19.828(2)
α, β, γ (deg)	90, 100.11(3), 90	109.440(1), 95.792(1), 90.752(1)	90, 106.221(1), 90	90, 98.653(4), 90	83.458(1), 73.203(1), 86.731(1)
vol (Å^3), Z	4184.4(14), 4	4372.4(1), 2	4468.6(2), 4	2190.9(2), 4	3369.2(6), 2
density (calc) (Mg/m^3)	1.64	1.56	1.43	1.71	1.63
absorption coeff (mm^{-1})	2.575	2.462	1.723	3.312	1.229
F(000)	2048	2024	1966	1112	1640
crystal size (mm^3)	0.15 × 0.08 × 0.05	0.30 × 0.22 × 0.15	0.18 × 0.15 × 0.05	0.12 × 0.07 × 0.02	0.06 × 0.06 × 0.05
θ range for data collectn (deg)	2.87−25.00	2.76−27.48	2.86−26.71	2.05−27.41	2.2−28.6
index ranges (h, k, l)	−13 to 13, −28 to 29, −18 to 18	−14 to 14, −24 to 24, −28 to 28	−15 to 18, −18 to 19, −26 to 24	−16 to 16, −16 to 16, −17 to 17	−17 to 17, −20 to 20, −28 to 28
no. of reflns collected	49113	67955	49199	9596	37981
no. of indep reflns/R_{int}	7357 (0.0982)	19922 (0.1780)	9784 (0.109)	9358 (0.0000)	19961 (0.0401)
completeness to θ_{max} (%)	99.8	99.4	99.4	99.0	99.2
absorption correction	semiempirical from equivs	semiempirical from equivs	semiempirical from equivs	semiempirical from equivs	semiempirical from equivs
max. and min. transmission	0.884 and 0.726	0.695 and 0.515	0.92 and 0.74	0.94 and 0.79	0.93 and 0.94
refinement method	full matrix least sq (F^2)	full matrix least sq (F^2)	full matrix least sq (F^2)	Full matrix least sq (F^2)	full matrix least sq (F^2)
no. data/restraints/params	7357/28/461	19922/46/821	6665/87/480	2917/344/235	19961/307/996
goodness-of-fit on F^2	1.053	1.008	1.099	0.987	1.041
final R indices [$I > 2\sigma(I)$]	R1 = 0.0437, wR2 = 0.0791	R1 = 0.0663, wR2 = 0.1484	R1 = 0.0834, wR2 = 0.0736	R1 = 0.0436, wR2 = 0.0456	R1 = 0.0575, wR2 = 0.1388
R indices (all data)	R1 = 0.0634, wR2 = 0.0849	R1 = 0.1390, wR2 = 0.1776	R1 = 0.1222, wR2 = 0.0857	R1 = 0.1439, wR2 = 0.2303	R1 = 0.0931, wR2 = 0.1571
largest peak/hole (e Å^{-3})	0.840 and −0.585	1.014 and −1.442	4.54 and −1.22	1.13 and −0.97	1.31 and −1.04

CH_3 of Cp*), 2.25 (m, 2H, CH_2), 3.25 (m, 2H, CH_2), 6.95 (m, 8H, CH aromatic), 7.15 (m, 8H, CH aromatic), 7.69 (m, 4H, CH aromatic). ^{13}C NMR (C_6D_6, 75 MHz): δ_C 9.4 (CH_3 of Cp*), 31.6 (dd, $^1J_{PC} = 15$, $^2J_{PC} = 8$ Hz, CH_2 of dppe), 85.2 (quaternary carbon of Cp*), 127.2 (aromatic CH), 127.3 (aromatic CH), 127.7 (aromatic CH), 129.3 (aromatic CH), 131.6 (aromatic CH), 131.8 (aromatic CH), 141.3 (d, $^1J_{PC} = 31$ Hz, *ipso* carbon of dppe), 141.7 (d, $^1J_{PC} = 31$ Hz, *ipso* carbon of dppe). ^{31}P NMR (C_6D_6, 122 MHz): δ_P 103.9. EI-MS, *m/z*: 911.9 {1%, $[Cp^*Fe(dppe)GaI_2]^+$}, 716.1 {22%, $[Cp^*Fe(dppe)I]^+$}, 589.2 {11%, $[Cp^*Fe(dppe)]^+$}, 398.2 {100%, $[dppe]^+$}. Exact mass: calc for $[Cp^*Fe(dppe)GaI_2]^+$ (i.e., M^+) 911.9216, meas. 911.9217. Elemental microanalysis. Calc for $\mathbf{3}\cdot{}^5/_4(C_7H_8)$: C, 52.27; H, 4.80. Meas.: C, 51.91; H, 4.35.

Reaction of $[Cp^*Fe(CO)_2GaI_2]_2$ (1) with dppe: Isolation of the Intermediate $Cp^*Fe(CO)(\mu_2\text{-dppe})GaI_2$ (2). To a solution of **1** (1.255 g, 1.100 mmol of dimer) in toluene (200 cm^3) was added a solution of dppe (0.986 g, 2.474 mmol) also in toluene (200 cm^3), and the reaction mixture was photolyzed for 70 h with periodic ^{31}P NMR monitoring. The resulting solution was filtered and concentrated in vacuo (to ca. 15 cm^3), and single crystals suitable for X-ray diffraction were obtained by layering a concentrated toluene solution with hexanes. Isolated yield 0.835 g, 40%. ^1H NMR (CD_2Cl_2, 300 MHz): δ_H 1.48 (s, 15H, CH_3 of Cp*), 1.95 (m, 2H, CH_2 of dppe), 2.55 (m, 2H, CH_2 of dppe), 7.10−7.49 (m, 16H, *ortho*- and *meta*-CHs of dppe), 7.68, 7.88 (m, each 2H, *para*-CH of dppe). ^{13}C NMR (CD_2Cl_2, 75 MHz): δ_C 8.7 (CH_3 of Cp*), 28.1 (d $^1J_{PC} = 15$ Hz, CH_2 of dppe), 28.3 (d $^1J_{PC} = 15$ Hz, CH_2 of dppe), 91.0 (quaternary carbon of Cp*), 124.5 (aromatic CH), 127.3 (aromatic CH), 128.0 (aromatic CH), 128.4 (aromatic CH), 129.5 (aromatic CH), 133.2 (aromatic CH), 134.0 (d $^1J_{PC} = 31$ Hz, *ipso* carbon of dppe), 134.2 (d $^1J_{PC} = 31$ Hz, *ipso* carbon of dppe), CO carbon not observed. ^{31}P NMR (CD_2Cl_2, 122 MHz): δ_P 65.0 (Fe−P), −41.0 (Ga−P). IR (CD_2Cl_2, cm^{-1}): ν(CO) 1981 (st). EI-MS, *m/z*: 939.7 {4%, $[Cp^*Fe(dppe)(CO)GaI_2]^+$}, 541.8 {19%, $[Cp^*Fe(CO)GaI_2]^+$}, 398.2 {67%, $[dppe]^+$}. Exact mass: calc. for $[Cp^*Fe(dppe)(CO)GaI_2]^+$ (i.e., M^+) 939.9165, meas. 939.9169. Reproducible microanalyses for crystalline samples of **2** proved impossible to obtain, possibly due to the presence of toluene within the crystal lattice.

$Cp^*Fe(dppe)Ga(Mes)I$ (4). To a solution/suspension of MesLi (0.036 g, 0.285 mmol) in toluene (25 cm^3) was added a solution of **3** (0.150 g, 0.164 mmol) also in toluene (15 cm^3), and the reaction mixture was stirred for 16 h at 20 °C. The resulting orange solution was filtered and concentrated (to ca. 10 cm^3), and **4** was obtained as an orange microcrystalline material on cooling to −30 °C. Crystals suitable for X-ray diffraction were obtained from a concentrated diethyl ether solution at −30 °C. Isolated yield 0.114 g, 71%. ^1H NMR (C_6D_6, 300 MHz): δ_H 1.42 (s, 15H, CH_3 of Cp*), 2.05 (m, 2H, CH_2 of dppe), 2.10 (s, 6H, *ortho*-CH_3 of Mes), 2.25 (s, 3H, *para*-CH_3 of Mes), 3.95 (m, 2H, CH_2 of dppe), 6.78 (s, 2H, CH of Mes), 7.02 (m, 4H, aromatic CH of dppe), 7.14−7.26 (m, 16H, aromatic ortho- and *meta*-CH of dppe), 7.80 (m, 4H, aromatic *para*-CH of dppe). ^{13}C NMR (CD_2Cl_2, 75 MHz): δ_C 10.3 (CH_3 of Cp*), 20.9 (*ortho*-CH_3 of Mes), 23.5 (*para*-CH_3 of Mes), 30.8 (dd $^1J_{PC} = 15.2$, $^2J_{PC} = 7.6$ Hz, CH_2 of dppe), 86.4 (quaternary carbon of Cp*), 127.2 (aromatic CH of dppe), 128.0 (aromatic CH of dppe), 128.9 (aromatic CH of dppe), 132.5 (aromatic CH of dppe), 133.5 (aromatic CH of dppe), 136.3 (aromatic CH of dppe), 139.3 (*ortho*-quaternary carbon of Mes), 139.4 (*meta*-CH of Mes), 141.0 (d $^1J_{PC} = 31.1$ Hz, *ipso*-carbon of dppe), 141.5 (d $^1J_{PC} = 31.1$ Hz, *ipso*-carbon of dppe), 142.5 (*para*-quaternary carbon of Mes). ^{31}P NMR (C_6D_6, 122 MHz): δ_P 99.0. EI-MS, *m/z*: 904 {1%, $[Cp^*Fe(dppe)Ga(Mes)I]^+$}, 777.1 {1%, $[Cp^*Fe(dppe)Ga(Mes)]^+$}, 716.0 {4%, $[Cp^*Fe(dppe)I]^+$}, 589.2 {9%, $[Cp^*Fe(dppe)]^+$}, 398.1 {49%, $[dppe]^+$}, 262.1 {42%, $[Cp^*FeGa]^+$}. Exact mass: calc. for $[Cp^*Fe(dppe)Ga(Mes)I]^+$ (i.e., M^+) 904.1032, meas. 904.1028. Reproducible microanalyses for crystalline samples of **4** proved impossible to obtain, possibly due to the presence of diethyl ether within the crystal lattice. **4** can also be prepared in an analogous manner using diethyl ether as the reaction solvent, albeit in lower yield (ca. 15%).

$Cp^*Fe(CO)_2Ga(Mes)I$ (5). To a solution of **1** (0.303 g, 0.266 mmol) in toluene (50 cm^3) was added a solution/suspension of MesLi (0.075 g, 0.595 mmol) also in toluene (40 cm^3), and the reaction mixture was stirred at 20 °C for 12 h. After filtration and removal of volatiles *in vacuo*, the resulting orange oil was extracted into diethyl ether (40 cm^3), concentrated (to ca. 15 cm^3), and cooled to −30 °C, yielding **5** as a pale yellow crystalline solid. Isolated yield 0.078 g, 26%. Crystals suitable for X-ray diffraction were obtained from a concentrated diethyl ether solution at −30 °C. ^1H NMR (CD_2Cl_2, 300 MHz): δ_H 1.13 (s, 15H, CH_3 of Cp*), 1.88 (s, 3H, *para*-Me of Mes), 2.09 (s, 6H, *ortho*-Me of Mes), 6.39 (s, 2H, CH of Mes). ^{13}C NMR (CD_2Cl_2, 75 MHz): δ_C 10.0 (CH_3 of Cp*), 21.5 (*para*-CH_3 of Mes), 22.7 (*ortho*-CH_3 of Mes), 95.2 (quaternary carbon of Cp*), 138.6 (*ortho*-quaternary carbon of Mes), 139.8 (*meta*-CH of Mes), 155.6 (*para*-quaternary carbon of Mes), 215.9 (CO), *ipso*-quaternary carbon of Mes not observed. IR (CD_2Cl_2, cm^{-1}): ν(CO) 1984 (st), 1936 (st). EI-MS, *m/z*: 562.0 {weak, $[Cp^*Fe(CO)_2Ga(Mes)I]^+$}, 534.0 {69%, $[Cp^*Fe(CO)Ga(Mes)I]^+$}, 506.0 {14%, $[Cp^*FeGa(Mes)I]^+$}, 435.1 {9%, $[Cp^*Fe(CO)_2Ga(Mes)]^+$}, 310.1 {100%, $[(OC)_2FeGaI]^+$}. Exact mass: calc. for $[Cp^*Fe(CO)_2Ga(Mes)I]^+$ (i.e., M^+) 561.9577, meas. 561.9581; calc. for $[Cp^*Fe(CO)Ga(Mes)I]^+$ [i.e., $(M - CO)^+$] 533.9628, meas. 533.9630. Elemental microanalysis. Calc. for **5**: C, 44.81; H, 4.66. Meas.: C, 49.22; H, 4.90.

$[CpFe(CO)_2]_2GaN(SiMe_3)_2$ (6) and $[Cp^*Fe(CO)_2]_2GaN(SiMe_3)_2$ (7). The two compounds were prepared in an analogous fashion, illustrated for **6**. To a slurry of $Na[CpFe(CO)_2]$ (0.442 g, 2.021 mmol) in diethyl ether was added a solution of $(Me_3Si)_2NGaCl_2\cdot THF$ (0.377 g, 1.011 mmol) also in diethyl ether (30 cm^3). The reaction mixture was stirred at 20 °C for 2 h, after which volatiles were removed *in vacuo*. The resulting yellow oil was dissolved in hexanes, filtered, concentrated (to ca. 20 cm^3), and cooled to −30 °C, yielding **6** as a pale yellow microcrystalline solid. Isolated yield: 0.421 g, 71%. ^1H NMR (C_6D_6, 300 MHz): δ_H 0.33 (s, 18H, CH_3 of $SiMe_3$), 4.21 (s, 10H, CH of Cp). ^{13}C NMR (C_6D_6, 75 MHz): δ_C 4.2 (CH_3 of $SiMe_3$), 82.6 (Cp), 215.9 (CO). IR (CD_2Cl_2, cm^{-1}): ν(CO) 1993 (st), 1972 (st), 1926 (st). EI-MS, *m/z*: 555.0 {23%, $[\{CpFe(CO)\}\{CpFe(CO)_2\}GaN(SiMe_3)_2]^+$}, 527.0 {4%, $[\{CpFe(CO)\}_2GaN(SiMe_3)_2]^+$}, 471.0 {17%, $[(CpFe)_2GaN(SiMe_3)_2]^+$}, 406.0 {100%, $[CpFe(CO)_2GaN(SiMe_3)_2]^+$}. Exact mass: calc. for $[\{CpFe(CO)\}\{CpFe(CO)_2\}GaN(SiMe_3)_2]^+$ [i.e., $(M - CO)^+$] 554.9557, meas. 554.9554. Data for **7**: crystals suitable for X-ray diffraction obtained from a concentrated diethyl solution at −30 °C. Isolated yield 0.543 g, 44%. ^1H NMR (C_6D_6, 300 MHz): δ_H 0.52 (s, 18H, CH_3 of $SiMe_3$), 1.57 (s, 30H, CH_3 of Cp*). ^{13}C NMR (C_6D_6, 75 MHz): δ_C 3.9 (CH_3 of $SiMe_3$), 9.2 (CH_3 of Cp*), 93.0 (quaternary carbon of Cp*), carbonyl carbon not observed. IR (CD_2Cl_2, cm^{-1}): ν(CO) 1973 (st), 1955 (st), 1908 (st). EI-MS, *m/z*: 695.1 {2%, $[\{Cp^*Fe(CO)\}\{Cp^*Fe(CO)_2\}GaN(SiMe_3)_2]^+$}, 476.1 {41%, $[Cp^*Fe(CO)_2GaN(SiMe_3)_2]^+$}, 420.1 {24%, $[Cp^*FeGaN(SiMe_3)_2]^+$}, 317.9 {31%, $[Cp^*Fe(CO)_2Ga]^+$}. Exact mass: calc. for $[\{Cp^*Fe(CO)\}\{Cp^*Fe(CO)_2\}GaN(SiMe_3)_2]^+$ [i.e., $(M - CO)^+$] 695.1122, meas. 695.1124. Elemental microanalysis. Calc. for **7**: C, 49.75; H, 6.68. Meas.: C, 50.11; H, 6.77.

$[Cp^*Fe(CO)_2Ga(Mes)(dtbpy)]^+[BAr^f{}_4]^-$ (8). A solution of **5** (0.094 g, 0.167 mmol) and dtbpy (0.045 g, 0.168 mmol) in CD_2Cl_2 (3 cm^3) was added to a slurry of $Na[BAr^f{}_4]$ (0.147 g, 0.166 mmol) in CD_2Cl_2 (1 cm^3) at −78 °C, and the reaction mixture was warmed to 20 °C. After sonication for 30 min, the resulting orange solution was layered with hexanes, yielding single crystals suitable for X-ray diffraction. Isolated yield 0.080 g, 31%. ^1H (300 MHz, CD_2Cl_2): δ_H 1.34 (s, 18H, ^{t}Bu of dtbpy), 1.76 (s, 15H, CH_3 of Cp*), 2.07 (s, 3H, *para*-CH_3 of Mes), 2.30 (s, 6H, *ortho*-CH_3 of Mes), 6.66 (s, 2H, CH of Mes), 7.46 (s, 4H, *para*-CH of $BAr^f{}_4^-$), 7.62 (s, 8H, *ortho*-CH of $BAr^f{}_4^-$), 7.72, 8.16, 8.75 (m, each 2H, CH of dtbpy). ^{13}C (75 MHz, CD_2Cl_2): δ_C 10.2 (Me of Cp*), 20.3 (*para*-CH_3 of Mes), 26.2 (*ortho*-CH_3 of Mes), 29.8 (^{t}BuCH_3 of dtbpy), 36.1 (^{t}Bu

Scheme 1. Contrasting Halide Abstraction Products from Three-Coordinate Boryl, Gallyl, and Indyl Ligand Systems[a]

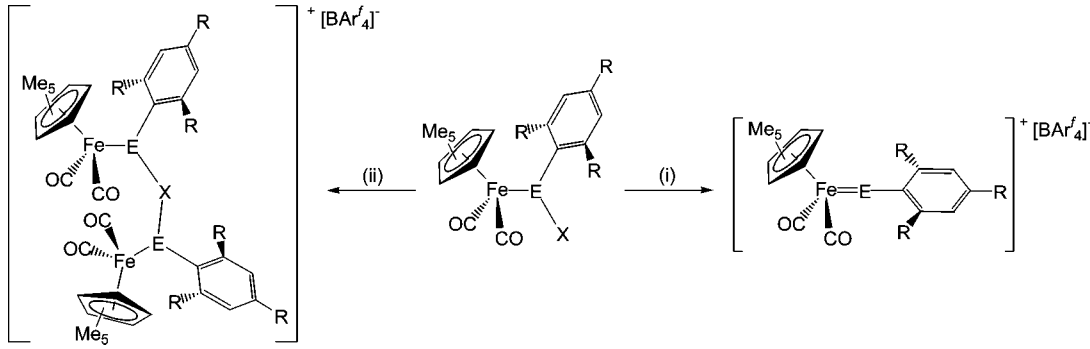

[a] Conditions: (i) Na[BAr$^f_4$], dichloromethane, E = B; R = Me; (ii) Na[BAr$^f_4$], dichloromethane, E = Ga, In; R = ^{t}Bu.

quaternary carbon of dtbpy), 95.5 (quaternary carbon of Cp*), 117.3 (CH of dtbpy), 117.4 (*para*-CH of BAr$^f_4{}^-$), 119.5 (CH of dtbpy), 122.7 (q $^1J_{CF}$ = 273 Hz, CF_3 of BAr$^f_4{}^-$), 124.7 (CH of dtbpy), 126.7 (quaternary carbon of dtbpy), 128.6 (q $^2J_{CF}$ = 29 Hz, *meta*-carbon of BAr$^f_4{}^-$), 134.8 (*ortho*-CH of BAr$^f_4{}^-$), 138.5 (*ortho*-quaternary carbon of Mes), 142.8 (*meta*-CH of Mes), 147.8 (quaternary carbon of dtbpy), 154.3 (*para*-quaternary carbon of Mes), 161.2 (q $^1J_{CB}$ = 49 Hz, *ipso*-carbon of BAr$^f_4{}^-$), 168.2 (quaternary carbon of dtbpy), 217.2 (CO), *ipso*-carbon of Mes not observed. ^{19}F (283 MHz, CD_2Cl_2): δ_F −62.9. ^{11}B (96 MHz, CD_2Cl_2): δ_B −8.4. IR (CD_2Cl_2, cm^{-1}): ν(CO) 1971 (st), 1919 (st). ES-MS, *m/z*: (10 V cone voltage) 703.2 {100%, [Cp*Fe(CO)$_2$-Ga(Mes)(dtbpy)]$^+$}; (50 V cone voltage) 703.2 {35%, [Cp*Fe-(CO)$_2$Ga(Mes)(dtbpy)]$^+$}, 435.0 {100%, [Cp*Fe(CO)$_2$Ga(Mes)]$^+$}. Exact mass: calc. for [Cp*Fe(CO)$_2$Ga(Mes)(dtbpy)]$^+$ 701.2519, meas. 701.2518. Elemental microanalysis. Calc. for **8**: C, 54.40; H, 3.99; N, 1.79. Meas.: C, 54.54; H, 4.12; N, 1.66.

[Cp*Fe(dppe)(GaI)]$^+$[BAr$^f_4$]$^-$ (9). To a suspension of Na-[BAr$^f_4$] (0.053 g, 0.060 mmol) in fluorobenzene (1 cm^3) at −30 °C was added an orange-red solution of **3** (0.049 g, 0.054 mmol) also in fluorobenzene (2 cm^3), and the reaction mixture was warmed to 20 °C over a period of 20 min. Monitoring of the reaction by ^{31}P{^{1}H} NMR spectroscopy revealed quantitative conversion of **3** (δ_P 103.9) to a single phosphorus containing species giving rise to a broad resonance at δ_P 87.0. The resulting deep violet solution was filtered and concentrated in *vacuo*, and purple crystals of **9** suitable for X-ray diffraction were obtained by layering with hexanes and storage at −30 °C. Analogous chemistry carried out in dichloromethane solution leads to the formation of a single species giving rise to a similar ^{31}P NMR resonance but which has a half-life of ca. 30 min at 20 °C. Isolated yield 0.031 g, 35%. ^{1}H NMR (C_6D_5F, 300 MHz): δ_H 1.18 (s, 15H, CH_3 of η^5-C_5Me_5), 1.88 (m, 2H, CH_2 of dppe), 2.04 (m, 2H, CH_2 of dppe), 7.14−7.37 (overlapping m, 20H, aromatic CH of dppe), 7.54 (s, 4H, *para*-CH of anion), 8.27 (s, 8H, *ortho*-CH of anion). ^{13}C NMR (C_6D_5F, 75 MHz): δ_C 9.2 (CH_3 of η^5-C_5Me_5), 31.5 (m, CH_2 of dppe), 86.5 (quaternary carbon of η^5-C_5Me_5), 117.0 (sept, J = 4.1 Hz, *para*-CH of anion), 124.3 (1:3:3:1 q, J = 272.1 Hz, CF_3 of anion), 128.0 (pseudo t, J = 4.6 Hz, *meta*-CH of dppe), 128.5 (1:3:3:1 q, J = 29.8 Hz, *meta*-carbon of anion), 129.1 (pseudo t, J = 5.1 Hz, *ortho*-CH of dppe), 130.0 (pseudo t, J = 4.6 Hz, *meta*-CH of dppe), 130.4 (*para*-CH of dppe), 130.8 (*para*-CH of dppe), 131.8 (pseudo t, J = 5.1 Hz, *ortho*-CH of dppe), 134.4 (*ortho*-CH of anion), 161.9 (1:1:1:1 q, J = 49.8 Hz, *ipso*-carbon of anion), *ipso*-carbons of dppe not observed. ^{11}B NMR (C_6D_5F, 96 MHz): δ_B 1.9. ^{19}F NMR (C_6D_5F, 282 MHz): δ_F −62.7. ^{31}P NMR (C_6D_5F, 122 MHz): δ_P 87.0. FT-Raman (C_6D_5F solution): ν(Ga−I) 186 cm^{-1}. UV/vis (C_6H_5F solution): λ_{max} = 549 nm; ε = 754 cm^{-1} mol^{-1} dm^3. ES-MS (positive ion mode), *m/z*: 785.0 {100%, [(η^5-C_5Me_5)Fe-(dppe)(GaI)]$^+$}, correct isotope pattern for $C_{36}H_{39}FeGaIP_2$. Exact mass: calc. for [(η^5-C_5Me_5)Fe(dppe)(GaI)]$^+$ (i.e., M$^+$) 785.0173, meas. 785.0204. Reproducible microanalyses for crystalline samples of **9** proved impossible to obtain, possibly due to the extreme sensitivity of this compound to air and moisture.

Reaction of 9 with CO: Formation of [Cp*Fe(dppe)(CO)]$^+$[BAr$^f_4$]$^-$ (12). A solution of **9** (0.050 g, 0.030 mmol) in d_5-fluorobenzene (2 cm^3) was exposed to CO gas (1 atm) at 20 °C for a period of 12 h, leading to a violet to yellow color change and to the formation of a gray precipitate. At this point, monitoring by ^{31}P NMR revealed quantitative conversion of **9** to a single phosphorus-containing species giving rise to a sharp signal at δ_P 88.0. Further analysis by ^{1}H and ^{13}C NMR, IR spectroscopy, and electrospray mass spectrometry, and comparison with literature data confirmed the presence of the [Cp*Fe(dppe)(CO)]$^+$ cation.[15]

Reaction of 9 with [^{n}Bu$_4$N]I: Formation of 3. To a solution of **3** (0.082 g, 0.050 mmol) in d_5-fluorobenzene (2 cm^3) was added a solution of [^{n}Bu$_4$N]I (0.022 g, 0.06 mmol) also in d_5-fluorobenzene with immediate formation of an orange solution and quantitative conversion of **9** to a single phosphorus-containing compound (δ_P 104.1). The identity of the product **3** was confirmed by comparison of ^{1}H, ^{13}C, and ^{31}P NMR data with those obtained from an authentic sample.

Results and Discussion

(i) Synthetic and Reactivity Studies. In previous work, we have shown that halide abstraction represents a valid synthetic approach to transition metal complexes containing low-coordinate group 13 ligands.[15–19] Extending the methodology pioneered for boron donors to the heavier elements of group 13, however, presents additional challenges. Thus, the greater size and metallic character of gallium and indium (cf. boron) are presumably responsible for the formation of halide-bridged dinuclear systems of the type [(η^5-C_5R_5)Fe(CO)$_2$E(Mes*)-(μ-X)(Mes*)EFe(CO)$_2$(η^5-C_5R_5)]$^+$ (E = Ga, In; X = Cl, Br; R = H, Me; Mes* = 2,4,6-^{t}Bu$_3$C$_6$H$_2$) by halide abstraction from (η^5-C_5R_5)Fe(CO)$_2$E(Mes*)X;[15d] by contrast, the two-coordinate terminal borylene system [Cp*Fe(CO)$_2$(=BMes)]$^+$ is obtained from the analogous reaction of Cp*Fe(CO)$_2$B(Mes)Br with Na[BAr$^f_4$] (Scheme 1).[15a]

In the case of cationic borylene complexes, the tendency of the unsaturated group 13 center to become trigonal by coordination of an additional two-electron donor can be reduced by incorporating sterically bulky π electron-donating substituents at boron (e.g., amino groups).[15e] While such an approach is also conceivable for the synthesis of analogous two-coordinate gallium-based ligand systems, an attractive alternative, which has achieved notable success in related group 14 chemistry, is the exploitation of sterically encumbered electron-rich *metal/ligand fragments*, L$_n$M. Synthetic studies designed to assess the relative merits of these two approaches are outlined below.

The dimeric species [Cp*Fe(CO)$_2$GaI$_2$]$_2$ (**1**) proves to be a versatile starting material for the exploration of cationic

Scheme 2. Syntheses of Precursor Complexes **3**−**5** from **1** via Gallium- and Iron-Centered Substitution Chemistries[a]

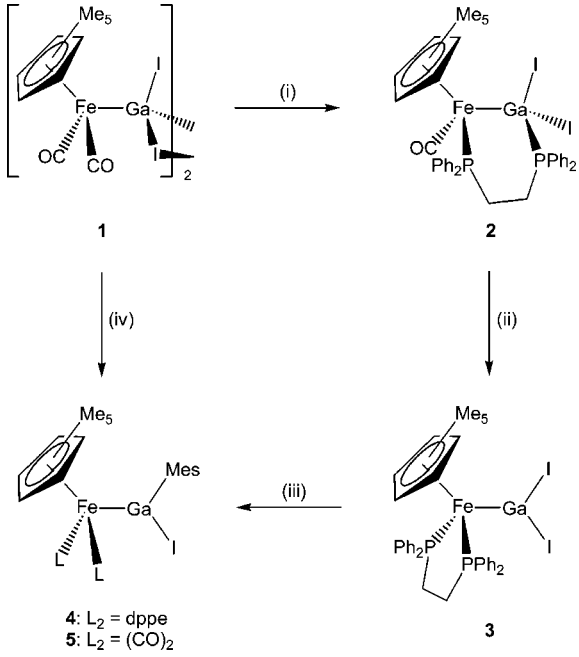

[a] Key reagents and conditions: (i) dppe (2.25 equiv per mol of dimeric **1**), toluene, 20 °C, UV photolysis for 70 h, 40% isolated yield; (ii) (from **1**) dppe (2.25 equiv per mol of dimeric **1**), toluene, 20 °C, UV photolysis for 86 h, 35% isolated yield; (iii) MesLi (1.73 equiv), toluene, 20 °C, 16 h, 77% isolated yield; (iv) MesLi (2.24 equiv per mol of dimeric **1**), toluene, 20 °C, 12 h, 26% isolated yield.

gallium−donor complexes (Scheme 2). **1** (and its ruthenium analogue **13**) is available in a one-pot process in multigram quantities from $[Cp^*M(CO)_2]_2$ (M = Fe, Ru), gallium metal, and iodine, and it is amenable to further functionalization at either the gallium or iron centers. Controlled functionalization at *gallium* to give unsymmetrically substituted gallyl derivatives such as the (monomeric) iodo(mesityl) complex $Cp^*Fe(CO)_2$-Ga(I)Mes (**5**) can be achieved in moderate yield, by substitution of a single iodide substituent with mesityllithium. Attempted substitution reactions with amido nucleophiles, $[NR_2]^-$, using **1** [or $Cp^*Fe(dppe)GaI_2$ (**3**), *vide infra*] as the gallium-containing substrate, however, proved unsuccessful.[30] Moreover, alternative approaches to complexes of the type $L_nMGa(X)NR_2$ exploiting the reactions of dihalo(amino)gallanes, R_2NGaX_2, with organometallic nucleophiles, generate instead disubstituted products of the type $[L_nM]_2GaNR_2$. Thus, the reactions of $[(\eta^5\text{-}C_5R_5)\text{-}Fe(CO)_2]^-$ (R = H, Me) with $(Me_3Si)_2NGaCl_2\cdot$THF lead to the formation of the bridging aminogallylene complexes $[(\eta^5\text{-}C_5R_5)Fe(CO)_2]_2GaN(SiMe_3)_2$ (**6**, R = H; **7**, R = Me), irrespective of reaction stoichiometry and conditions.[31] Further attempts to manipulate the substituent at gallium, beyond simple halo or aryl derivatives, were therefore ignored (and ultimately proved to be unnecessary), with attention focusing instead on manipulation of the steric/electronic properties of the metal fragment, L_nM.

Electron-rich group 8 metal fragments containing bulky cyclopentadienyl and tertiary phosphine ligands have been shown to be compatible with highly electrophilic ligands such as base-free dialkyl silylenes.[32] On this basis, we targeted similar metal/ligand combinations to provide the steric and electronic protection necessary to isolate a cationic terminal gallylene complex. Furthermore, we identified photolytic carbonyl substitution chemistry at the gallyl precursor stage as a potential route to the desired metal/ligand combinations.[33] In the event, and somewhat counterintuitively, dppe [1,2-bis(diphenylphosphino)ethane] proves to be an ideal phosphine ancillary ligand (on the basis of optimal steric shielding of the gallium fragment by the pendant phenyl rings, *vide infra*) and iron (rather than ruthenium) the metal of choice.[34] Reaction of the readily available dicarbonyl substituted precursor **1** with dppe in toluene can be shown by a combination of ^{31}P NMR and X-ray crystallography to proceed via a monocarbonyl intermediate (**2**) in which the dppe ligand bridges in an intramolecular fashion between the iron and gallium centers (Scheme 2). Particularly diagnostic are the two ^{31}P resonances measured for **2**; that at δ_P −41 is similar to other gallyl/dppe Lewis acid/base complexes {cf. δ_P −28.0 for $[(\eta^7\text{-}C_7H_7)Mo(CO)_2GaI_2]_2(\mu\text{-dppe})$},[33] while that at δ_P 65 is consistent with dppe bound to iron in a nonchelating fashion [cf. δ_P 70.3 and 75.9 for CpFe(CO)-(COMe)(μ-dppe)Fe$(CO)_2(\eta^4\text{-}C_5H_4Me)$].[35] Prolonged photolysis results in the disappearance of the signal due to **2**, with accompanying growth of the single resonance (δ_P 104) associated with the final chelating dppe product.[36] Multinuclear NMR, mass spectrometry, analytical, and X-ray crystallographic data

(30) Work on related systems has shown that metallated trihalogallates, $[L_nMGaX_3]^-$, are among the products of such reactions with bulky amide reagents, typically isolated as the $[R_2NH_2]^+$ salts. See, ref 8a and: Aldridge, S.; Kays, D. L.; Bunn, N. R.; Coombs, N. D.; Ooi, L.-L. *Main Group Met. Chem.* **2005**, *28*, 201.

(31) Such reactivity mirrors analogous chemistry toward the sterically encumbered dichloro*borane* $(Me_3Si)_2NBCl_2$, which generates a bridging aminoborylene complex, irrespective of reaction conditions: Braunschweig, H.; Kollann, C.; Englert, U. Eur. J. Inorg. Chem. 1998, 465.

(32) See, for example: (a) Grumbine, S. K.; Tilley, T. D.; Arnold, F. P.; Rheingold, A. L. *J. Am. Chem. Soc.* **1994**, *116*, 5495. For a discussion of the use of related electron rich metal/ligand frameworks in stabilizing dihalocarbene ligands, see, for example: (b) Brothers, P. J.; Roper, W. R. *Chem. Rev.* **1988**, *88*, 1293.

(33) Potential syntheses, such as insertion of gallium(I) reagents into the metal−halogen bonds of bis(phosphine) metal halides [e.g. of the type $(\eta^5\text{-}C_5R_5)Ru(PR_3)_2X$] have previously been shown to generate alternative tetrahalogallate products of the type $(\eta^5\text{-}C_5R_5)Ru(PR_3)_2(GaX_4)$ containing no direct Ru−Ga bonds: (a) Coombs, N. D.; Stasch, A.; Aldridge, S. *Inorg. Chim. Acta* **2008**, *361*, 449.

(34) Although enhanced back-bonding to the putative EX ligand might identify ruthenium (or osmium) containing systems as more viable targets—in line with classical bonding models—this same factor is presumably responsible for the much less facile carbonyl ligand substitution chemistry observed for gallyl precursors containing ruthenium. The reaction chemistry between dppe and $[Cp^*Ru(CO)_2GaI_2]_2$ (**13**) is consistent with significantly higher barriers to carbonyl substitution than observed for $[Cp^*Fe(CO)_2GaI_2]_2$ (**1**). Thus, although a compound with ^{31}P NMR signals at δ_P 44 and −40, similar to those measured for $Cp^*Fe(CO)(\mu_2\text{-dppe})GaI_2$ (**2**; δ_P 65 and −41), is observed in low concentration at short reaction times, $Cp^*Ru(dppe)GaI_2$ is not identified among the reaction components at any time. The dppe-bridged dinuclear species $[Cp^*Ru(CO)_2GaI_2]_2(\mu\text{-dppe})$ (**14**) is the only Ru/Ga/P containing product isolated from the toluene reaction mixture after 60 h, while the formation of appreciable quantities of $Cp^*Ru(dppe)I$ (**15**) and the known cation $[Cp^*Ru(dppe)(CO)]^+$ (**16**) at extended reaction times testifies to the lability of the gallyl ligand under conditions which are sufficiently forcing to effect carbonyl substitution chemistry (see Supporting Information for synthetic, spectroscopic, and crystallographic data). $[Cp^*Ru(dppe)(CO)]^+$: (a) Bruce, M.; Ellis, B. G.; Skelton, B. W.; White, A. H. *J. Organomet. Chem.* **2005**, *690*, 792.

(35) Luh, L.-S.; Liu, L.-K. *Organometallics* **1995**, *14*, 1514.

(36) A similar mechanism has been proposed by Ueno and co-workers for related dmpe [1,2-bis(dimethylphosphino)ethane] chemistry on the basis of spectroscopic data, albeit without structural characterization: (a) Ueno, K.; Hirotsu, M.; Hatori, N. *J. Organomet. Chem.* **2007**, *692*, 88.

Scheme 3. Formation of the Base-Stabilized Cationic Gallylene **8** by Halide Abstraction in the Presence of dtbpy Trapping Agent[a]

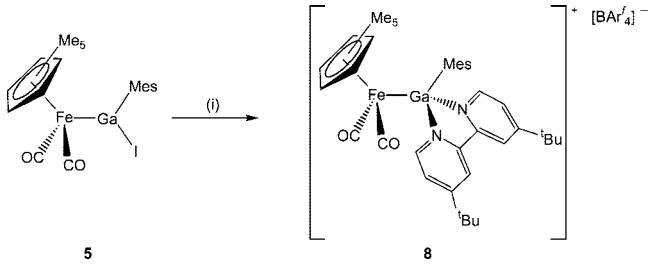

[a] Key reagents and conditions: (i) Na[BAr$^f_4$] and dtbpy (1.0 equiv of each), d_2-dichloromethane, 20 °C, 30 min of sonication, 31% isolated yield.

are consistent with this species being the expected product Cp*Fe(dppe)GaI$_2$ (**3**) isolated from toluene solution in ca. 35% yield. As with **1**, further substitution chemistry at the gallium center in **3** can be achieved cleanly with MesLi (ca. 2 equiv) in diethyl ether or with improved yields (ca. 70%) in toluene; Cp*Fe(dppe)Ga(Mes)I (**4**) has been characterized by standard spectroscopic techniques, and its structure in the solid state has been confirmed by single crystal X-ray diffraction studies.

The success of subsequent halide abstraction chemistry in delivering tractable terminal gallylene complexes from halogallyl precursors **3**−**5** can readily be demonstrated but is strongly dependent on the nature of the metal- and gallium-bound substituents, the halide abstraction agent, and the solvent used (*vide infra*).[37] Given the appropriate choice of counterion (typically the weakly coordinating anion [BAr$^f_4$]$^-$), the nature of the metal-bound ancillary ligands appears to be the key factor in determining complex stability. In previous studies, we have shown that halide abstraction, even from relatively bulky halogallyl ligands such as -Ga(Mes*)X, invariably leads to the formation of halide-bridged dinuclear products if partnered with a transition metal fragment of the type [(η^5-C$_5$R$_5$)Fe(CO)$_2$].[38] Indeed, in our hands, the isolation of *mononuclear* cationic species can only be achieved by carrying out such abstraction reactions in the presence of a suitable trapping agent, such as a chelating bipyridyl ligand (Scheme 3). Thus, iodide abstraction from Cp*Fe(CO)$_2$Ga(Mes)I (**5**) in the presence of dtbpy leads to the formation of [Cp*Fe(CO)$_2$Ga(Mes)(dtbpy)]$^+$[BAr$^f_4$]$^-$ (**8**) as yellow acicular crystals in ca. 30% isolated yield. The composition of **8** has been established by standard spectroscopic and analytical techniques and by comparison with related species reported by Ueno and Ogino.[39] Most informative, though, are the results obtained by positive-ion electrospray mass spectrometry (Figure 1). Thus, at a relatively low cone voltage (10 V) a "flagpole"mass spectrum corresponding to the molecular ion of the dtbpy adduct [Cp*Fe(CO)$_2$Ga(Mes)(dtbpy)]$^+$is observed, while at higher voltages (ca. 50 V) the predominant isotopic envelope (centered at *m*/*z* 435.0) corresponds to the base-free cationic gallylene [Cp*Fe(CO)$_2$(GaMes)]$^+$. While such spectra do not necessarily offer any encouragement for the isolation of CO-ligated species in *macroscopic* quantities, they do at least provide the first spectroscopic evidence for the cationic gallium−donor analogue of [Cp*Fe(CO)$_2$(=BMes)]$^+$ [15a] and an indication that the Fe−Ga bond is retained, at least for the isolated compound in the gas phase.

In terms of isolating the desired base-free terminal gallylene systems in quantities suitable for spectroscopic and structural characterization, the use of more electron rich and sterically shielded metal/ligand fragments appears to be crucial. Thus, although the reaction of Cp*Fe(dppe)Ga(Mes)I (**4**) with Na[BAr$^f_4$] does not lead to the isolation of any tractable Fe−Ga containing products, reaction of Cp*Fe(dppe)GaI$_2$ (**3**) with the same halide abstraction agent generates [Cp*Fe(dppe)(GaI)]$^+$[BAr$^f_4$]$^-$ (**9**) in 35% isolated yield (see Scheme 4). In the case of **3**, the reaction proceeds quantitatively in fluorobenzene solution (as evidenced by ^{31}P NMR monitoring or by ^{1}H NMR monitoring in d_5-fluorobenzene) to a single phosphorus- and Cp*-containing compound; the lower isolated yield presumably reflects losses associated with the recrystallization of this extremely air- and moisture-sensitive material. Crystallization from a mixture of fluorobenzene and hexanes (ca. 1:10) at −30 °C leads to the isolation of violet crystals of **9**, the constitution of which has been unambiguously established by a combination of multinuclear (^{1}H, ^{11}B, ^{13}C, ^{19}F, and ^{31}P) NMR, UV/vis, and FT-Raman spectroscopies, electrospray mass spectrometry (including exact mass measurement), and single crystal X-ray diffraction. Particularly informative are the positive ion electrospray mass spectra obtained for **9** in fluorobenzene solution (see Figure 2). In addition to providing definitive identification of the molecular ion by isotopic profiling (Figure 2a), fragmentation data reveal the presence of the coordinated GaI ligand. Thus, MS-MS experiments performed on the molecular ion are consistent with ready fragmentation generating the [Cp*Fe(dppe)]$^+$ cation by loss of GaI (Figure 2b). Facile dissociation of the GaI ligand from **9** is also consistent with the results of chemical and computational experiments (*vide infra*).

Attempts to isolate **9** from the corresponding reaction in dichloromethane lead instead to the formation of paramagnetic products. Monitoring of the reaction mixture by ^{31}P NMR reveals initial conversion of **3** to a single species which gives rise to a broad resonance at a very similar chemical shift (δ_P 87.0) to that observed for the analogous reaction in fluorobenzene solution (together with a similar red to violet color change). In dichloromethane solution this signal has a half-life of ca. 30 min at 20 °C; after several hours the solution is typically brown in color and exhibits no discernible ^{31}P resonances. Tilley has previously shown that cationic osmium silylene complexes react with chlorocarbons via chlorine atom abstraction,[40] and we were successful in isolating and structurally characterizing the 17-electron [Cp*Fe(dppe)Cl]$^+$ cation by layering of the dichloromethane reaction mixture with hexanes {as the [BAr$^f_4$]$^-$ salt (**11**); see the Supporting Information}. In common with related cationic borylene complexes, **9** also shows evidence of both gallium- and iron-centered reactivity toward nucleophiles. Thus,

(37) The use of commercially available but more reactive counterions such as [BPh$_4$]$^-$ or [BF$_4$]$^-$ typically leads to products containing Fe-Ph, or *E*(μ-F)E moieties (E = Ga, In); the [BAr$^f_4$]$^-$ anion is typically found to be more weakly interacting, although under appropriate conditions it too can act as a source of fluoride toward very strongly electrophilic cations: (a) Kays, D. L.; Rossin, A.; Day, J. K.; Ooi, L.-L.; Aldridge, S. *Dalton Trans.* **2006**, 399. (b) Coombs, D. L.; Aldridge, S.; Rossin, A.; Jones, S.; Willock, D. J. *Organometallics* **2004**, *23*, 2911. (c) Buschmann, W. E.; Miller, J. S. *Chem.*−*Eur. J.* **1998**, *4*, 1731. (d) Hughes, R. P.; Husebo, T. L.; Maddock, S. M. *J. Am. Chem. Soc.* **1997**, *119*, 10231. (e) Ferraris, D.; Cox, C.; Anand, R.; Lectka, T. *J. Am. Chem. Soc.* **1997**, *119*, 4319. (f) Bahr, S. R.; Boudjouk, P. *J. Am. Chem. Soc.* **1993**, *115*, 4514.

(38) Reaction of Na[BAr$^f_4$] with [Cp*M(CO)$_2$GaI$_2$]$_2$ (**1**, M = Fe; **13**, M = Ru) can be shown to proceed to the generation of the iodide-bridged cations [{Cp*M(CO)$_2$}$_2$(μ-I)]$^+$ (**10**, M = Fe; **17**, M = Ru) as the [BAr$^f_4$]$^-$ salts (see Supporting Information for details).

(39) Ueno, K.; Watanabe, T.; Ogino, H. *Appl. Organomet. Chem.* **2003**, *17*, 403.

(40) Wanandi, P.; Glaser, P. B.; Tillet, T. D. *J. Am. Chem. Soc.* **2000**, *122*, 972.

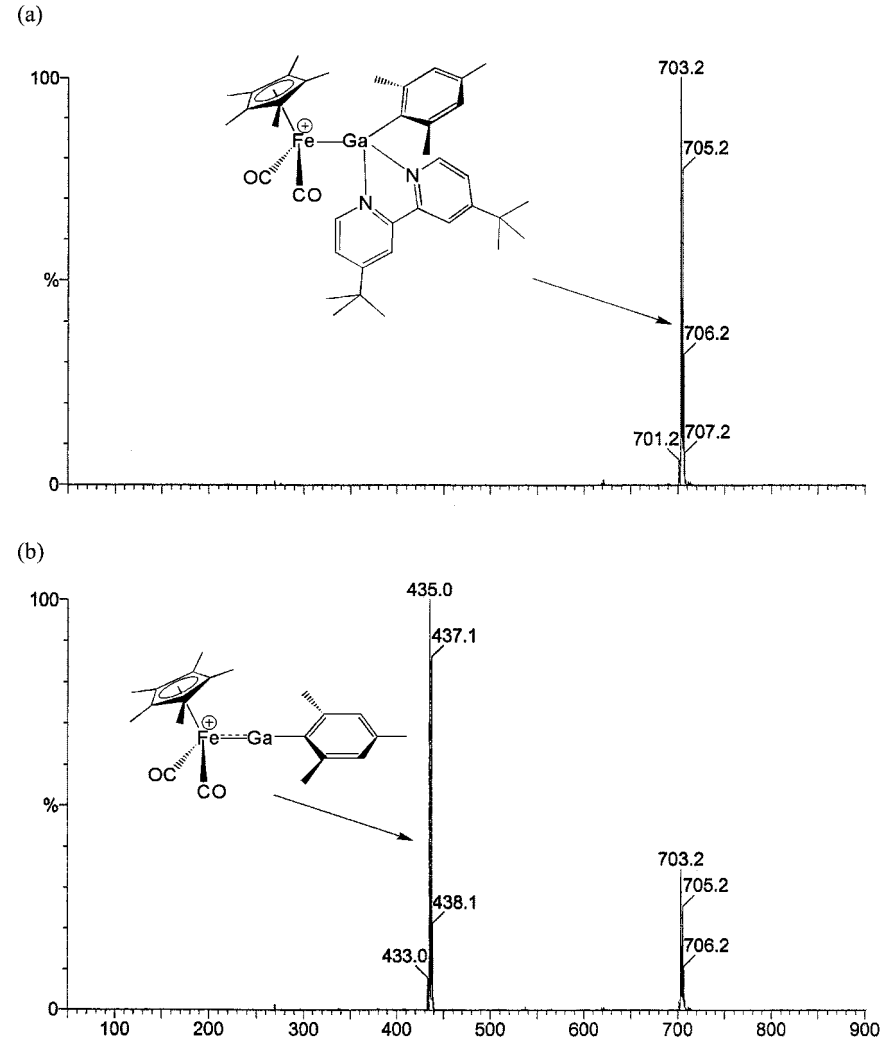

Figure 1. Positive ion electrospray mass spectra of **8**: (a) cone voltage 10 V; (b) cone voltage 50 V.

Scheme 4. Synthesis and Reactivity of Cationic Iodogallylene Complex **9**[a]

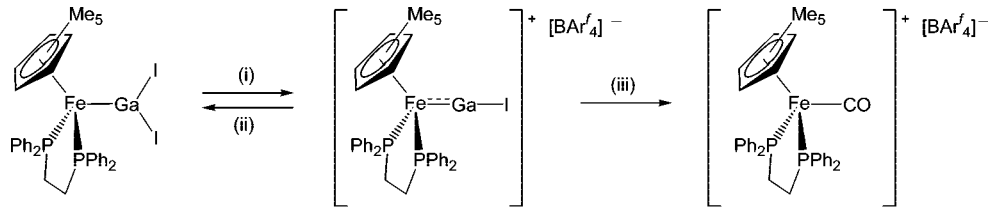

[a] Key reagents and conditions: (i) Na[BAr$^f_4$] (1.11 equiv), fluorobenzene, −30 to 20 °C, 20 min, 35% isolated yield; (ii) [^{n}Bu$_4$N]I (1.2 equiv), d_5-fluorobenzene, 20 °C, 5 min, quantitative by NMR; (iii) CO (1 atm), d_5-fluorobenzene, 20 °C, 12 h, quantitative by NMR.

reaction with [^{n}Bu$_4$N]I in fluorobenzene solution proceeds rapidly via addition of iodide at the gallium center and simple (quantitative) regeneration of the diiodogallyl precursor complex **3**. Reaction with carbon monoxide, on the other hand, can be shown by IR and multinuclear NMR spectroscopies to proceed via ligand displacement at the iron center, with the corresponding carbonyl complex [Cp*Fe(dppe)(CO)]$^+$[BAr$^f_4$]$^-$ being generated in quantitative yield (by NMR) over a period of ca. 20 h; gallium metal is precipitated during the course of the reaction. The course of this reaction can be understood by recourse to DFT calculations carried out for **9** and [Cp*Fe(dppe)(CO)]$^+$ (*vide infra*) which reveal a significantly stronger metal ligand bond for CO vs GaI; gallium metal presumably results from the disproportionation of the ejected GaI moiety.

(ii) Structural Studies. The structures of precursor iodogallyl complexes **2**−**5** and of cationic iodogallylene **9** have been determined in the solid state by X-ray crystallography (see Figures 3 and 4), and they imply a crucial role for ancillary ligand steric shielding in the stabilization and geometric properties of low-coordinate gallium centers. Thus, in contrast to the dimeric structure adopted by the corresponding dicarbonyl complex [Cp*Fe(CO)$_2$GaI$_2$]$_2$ (**1**),[8a] the structure of Cp*Fe(dppe)GaI$_2$ (**3**) is monomeric and features a trigonal gallium center [$\sum$(angles at gallium) = 360°, within the standard 3σ

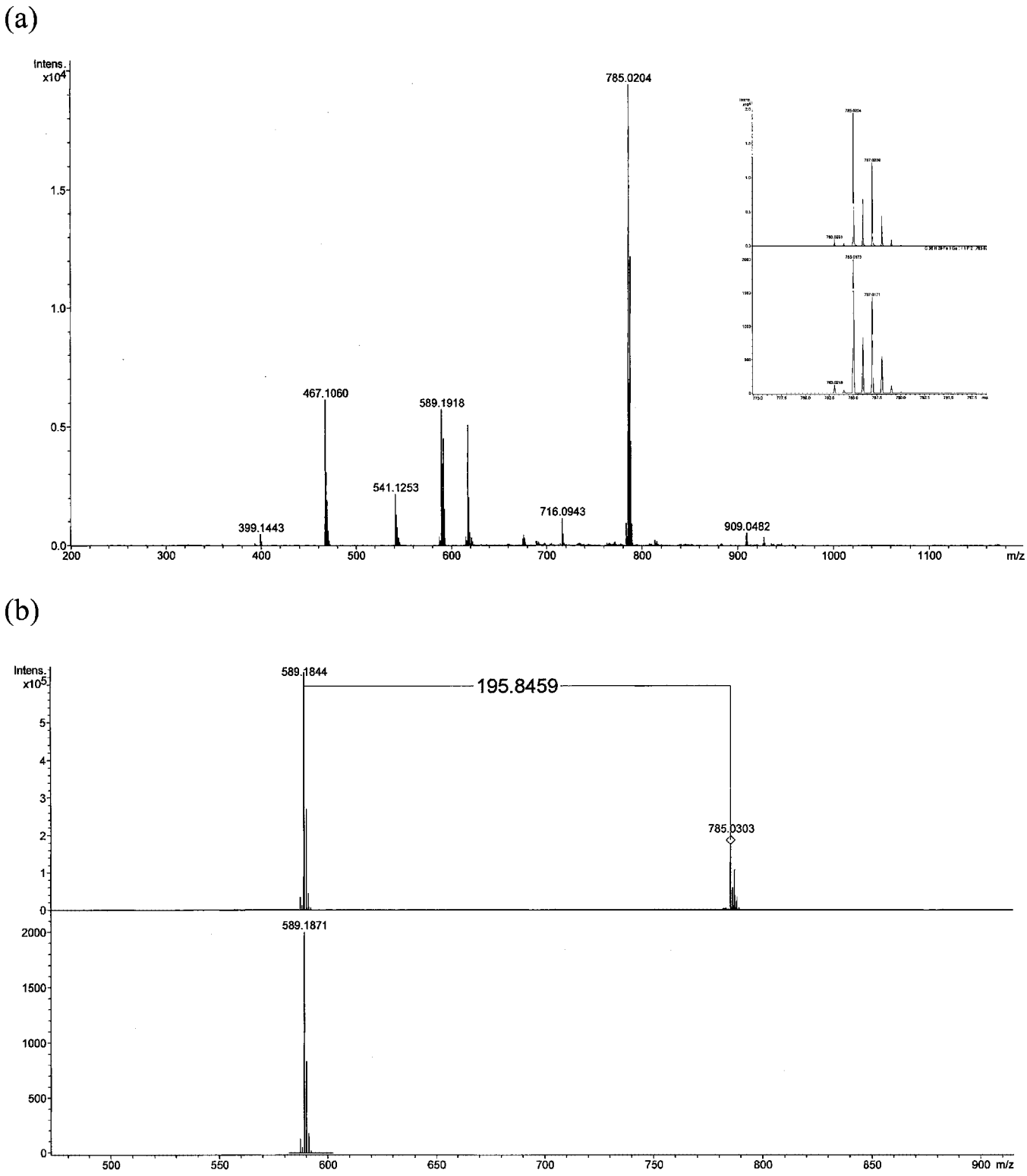

Figure 2. (a) Positive ion electrospray mass spectrum of **9**; (inset) calculated and measured isotopic envelopes for the molecular ion. (b) (upper) Positive ion MS/MS spectrum of the molecular ion of **9** showing formation of the $[Cp^*Fe(dppe)]^+$ fragment by loss of GaI (mass 195.8459); (lower) calculated isotopic envelope for $[Cp^*Fe(dppe)]^+$.

limit]. While such three-coordinate complexes (of the type L_nMEX_2) are more common for E = B, **3** represents a very rare example of such a ligand system incorporating one of the heavier group 13 elements.[41] The steric bulk of the chelating dppe ligand is clearly of key importance, with the consequence that the Fe−Ga distances for **3** [2.3236(14) and 2.3201(14) Å, for the two distinct molecules in the asymmetric unit] are actually slightly *longer* than that measured for **1** [2.314(1) Å] despite the lower coordination number at gallium (three vs four);[8a] further lengthening of the Fe−Ga bond is observed for Cp*Fe(dppe)Ga(Mes)I [**4**; 2.355(1) Å]. Moreover, an informative illustration of the relative importance of steric and electronic factors can be obtained by comparison of the structures of iodo(mesityl) complexes $Cp^*Fe(L)_2Ga(Mes)I$ [**4**: L_2 = dppe; **5**: $L_2 = (CO)_2$] which

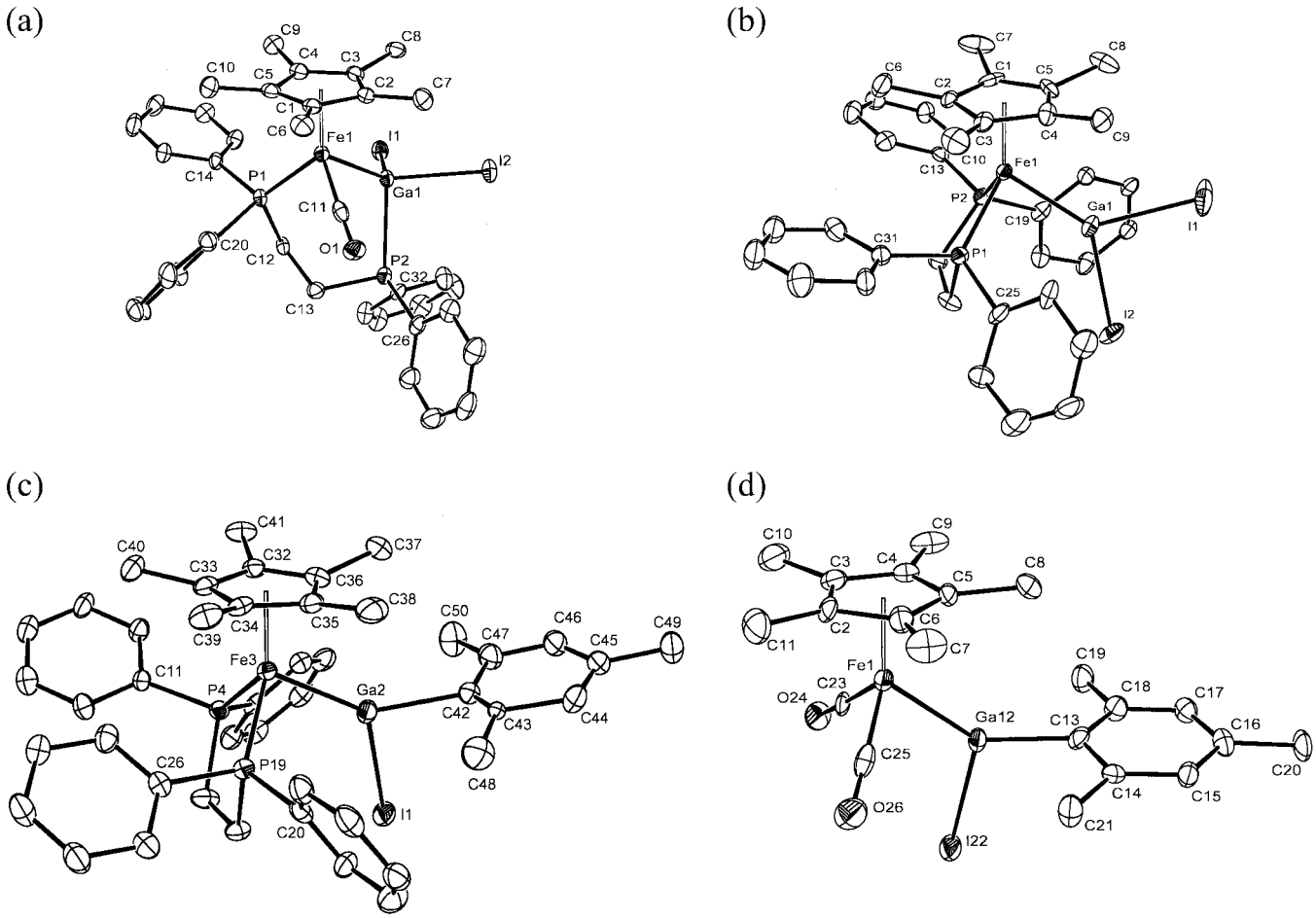

Figure 3. Molecular structures of halogallyl complexes (a) **2**, (b) **3**, (c) **4**, and (d) **5** with hydrogen atoms omitted for clarity and atomic displacement ellipsoids set at the 50% probability level. Key bond lengths (Å) and angles (deg): (for **2**) Fe(1)−Ga(1) 2.3558(10), Fe(1)−P(1) 2.2107(13), Ga(1)−I(1) 2.6855(7), Ga(1)−I(2) 2.6416(8), Ga(1)−P(2) 2.5288(12), I(1)−Ga(1)−I(2) 97.80(2); (for **3**) Fe(1)−Ga(1) 2.3236(14), Fe(1)−P(1) 2.193(2), Fe(1)−P(2) 2.208(2), Ga(1)−I(1) 2.6294(11), Ga(1)−I(2) 2.6323(11), P(1)−Fe(1)−P(2) 86.88(9), Fe(1)−Ga(1)−I(1) 131.67(5), Fe(1)−Ga(1)−I(2) 134.02(5), I(1)−Ga(1)−I(2) 94.30(4), angle between least-squares planes defined by [Cp* centroid, Fe(1), Ga(1)] and [Ga(1), I(1), I(2)] 16.78; (for **4**) Fe(3)−Ga(2) 2.355(1), Fe(3)−P(4) 2.192(2), Fe(3)−P(19) 2.186(2), Ga(2)−I(1) 2.726(1), Fe(3)−Ga(2)−C(42) 140.0(2), Fe(3)−Ga(2)−I(1) 127.54(4), I(1)−Ga(1)−C(42) 91.3(2), angle between least-squares planes defined by [Cp* centroid, Fe(3), Ga(2)] and [Ga(2), I(1), C(42)] 14.14, angle between least-squares planes defined by [Ga(2), I(1), C(42)] and [C(42) to C(47)] 82.87; (for **5**) Fe(1)−Ga(12) 2.3113(12), Ga(12)−I(22) 2.6073(9), Fe(1)−Ga(12)−C(13) 137.20(19), Fe(1)−Ga(12)−I(22) 116.86(4), C(13)−Ga(12)−I(22) 105.16(18), angle between least-squares planes defined by [Cp* centroid, Fe(1), Ga(12)] and [Ga(12), C(13), I(22)] 13.11, angle between least-squares planes defined by [Ga(12), C(13), I(22)] and [C(13) to C(18)] 89.71.

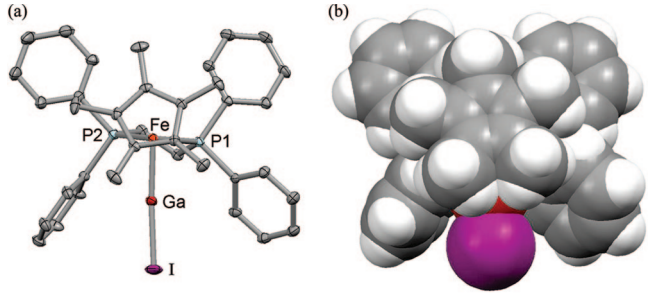

Figure 4. (a) Molecular structure of the major (79%) component of $[Cp^*Fe(dppe)(GaI)]^+[BAr^f_4]^-$ (**9**) as determined by single crystal X-ray diffraction studies. Counterion and hydrogen atoms omitted for clarity, and atomic displacement ellipsoids drawn at the 50% probability level. Key bond lengths and angles: Fe−Ga, 2.2221(6) Å; Ga−I, 2.4436(5) Å; Fe−P(1), 2.2068(9) Å; Fe−P(2), 2.2199(10) Å; Fe−Ga−I, 171.37(3)°; P(1)−Fe−P(2), 86.60(3)°; P(1)−Fe−Ga, 86.16(3)°; P(2)−Fe−Ga, 91.02(3)°. (b) Space filling diagram of the cationic component of **9**. Color key: gray (carbon), white (hydrogen), blue (phosphorus), red (gallium), purple (iodine).

feature similar alignments of the gallyl ligand and which differ only in the ancillary ligand framework at the iron center. That a much longer Fe−Ga bond [2.355(1) vs 2.3113(12) Å] and a significantly wider Fe−Ga−C_{ipso} angle [140.0(2) vs 137.20(19)°] are found for dppe-ligated **4** implies that the extra steric demands of the chelating phosphine predominate over any potential increase in Fe → Ga back-bonding.

The structure of **9** determined crystallographically in the solid state is shown in Figure 4. Disorder within the structure is successfully modeled in terms of two cationic species; the major component (79%) features discrete $[Cp^*Fe(dppe)(GaI)]^+$ and $[BAr^f_4]^-$ ions, with no short secondary interactions involving the Fe−Ga−I unit (within standard van der Waals contacts). Key structural features are the essentially linear arrangement of the iron, gallium, and iodine atoms [∠Fe−Ga−I = 171.37(3)°] typical of a terminally bound diatomic ligand {cf. ∠Fe−C−O = 175.8(5)° for $[Cp^*Fe(dppe)(CO)]^+[PF_6]^-$},[20b] and the extremely short Fe−Ga and Ga−I distances [2.2221(6) and 2.4436(5) Å, respectively]. The gallium−iodine distance is the shortest yet reported; likewise, the metal−gallium distance, is among the shortest yet reported involving *any* transition metal

(41) Buchin, B.; Gemel, C.; Kempter, A.; Cadenbach, T.; Fischer, R. A. *Inorg. Chim. Acta* **2006**, *359*, 4833.

Table 2. Energy Partitioning Analyses for the Model Complexes $[CpFe(dmpe)(EX)]^+$ (EX = N_2, CO, BF, and GaI)[48]

	N_2	CO	BF	GaI
dipole moment (Debye)[a]	0 (0)	0.047 (0.138)	0.884 (0.971)	1.866 (3.818)
quadrupole moment (au)	−1.036	−1.459	−3.533	−13.327
Pauli repulsion (ΔE_{Pauli}, kJ mol^{-1})	374	623	842	367
electrostatic interaction ($\Delta E_{electrostat}$, kJ mol^{-1})	−232	−439	−658	−234
orbital interaction (ΔE_{orb}, kJ mol^{-1})	−262	−397	−469	−236
total interaction energy (ΔE_{int}, kJ mol^{-1})	−120	−213	−285	−103
π contribution to covalent bonding density (%)	38	39	42	33

[a] Dipole moments quoted are for the ligands in the geometries they have in the complex; those in parentheses are for the isolated ligands.

(and the shortest involving iron).[5,42] With due allowance made for the differing radii of Fe(II) and Ni(II) (0.82 and 0.78 Å),[9] the M−Ga distance measured for **9** is comparable to that found by Uhl and co-workers for the homoleptic diyl system Ni[GaC(SiMe$_3$)$_3$]$_4$ [2.1700(4) Å].[42] Structural evidence for **9** also points to ready bending deformation of the Fe−Ga−I bond, viz. large thermal ellipsoid amplitude for the iodine atom perpendicular to the Fe−Ga−I axis. Secondary off-axis electron density has been modeled as a minor (21%) cationic component featuring a markedly more bent Fe−Ga−I unit [148.92(5)°] and contacts between I′ and C(55)−C(58) of one of the $[BAr^f_4]^-$ aromatic rings which fall within the sum of the van der Waals radii of iodine and carbon. Large librational amplitudes at oxygen in related metal carbonyl complexes are often associated with analogous Fe−C−O bending motions, and the ready deformation of the linear Fe−Ga−I fragment in **9** (and a small calculated energy difference between the linear and bent geometries) is consistent with the smaller absolute magnitude of directional covalent contributions to the metal ligand bond (*vide infra*).

A contributory factor to the short bond lengths in **9** is the low coordination number at gallium. Thus, short Fe−Ga bonds are also associated with the two-coordinate gallium centers in (OC)$_4$FeGaAr [Ar = C$_6$H$_3$(C$_6$H$_2$^{i}Pr$_3$)$_2$-2,6; d(Fe−Ga) = 2.2248(7) Å],[22a] Cp*Fe(dppe)GaFe(CO)$_3$L [e.g., d(Fe−Ga) = 2.248(1) for L = CO],[21] and [{Cp*Fe(CO)$_2$}$_2$Ga]$^+$ [d(Fe−Ga) = 2.272(1) and 2.266(1) Å],[15b] while longer bonds are measured for the three-coordinate precursor **3** [d(Fe−Ga) = 2.322 Å (mean); d(Ga−I) = 2.631 Å (mean)] and for the four coordinate system $[Cp^*Fe(CO)_2GaCl(phen)]^+$ [d(Fe−Ga) = 2.3047(4) Å; phen = 1,10-phenanthroline].[39,43] Potentially, a second factor underlying these short bonds is the presence of off-axis electronic contributions to the bonding, involving gallium-based orbitals of π symmetry. The contraction of the Fe−Ga bond on halide abstraction (ca. 4.3% for **9** compared to **3**) is markedly less than that for analogous boron-containing systems (typically 9−10%),[15] for which descriptions incorporating Fe═B π bonds have been advanced for the cationic products. That said, smaller changes in bond length as a function of bond order are typically found for the heavier main group elements,[44] and the Fe−Ga contraction between **9** and **3** mirrors that found between double and single bonds involving the adjacent group 14 element germanium (e.g., 4.7% between Mn−Ge and Mn═Ge bonds).[45] In order to better understand the bonding in the unprecedented ligand system present in **9** and to provide comparison of group 13/17 EX ligands with group 14/16 and group 15/15 counterparts, an in-depth computational investigation of the bonding in **9** and related complexes was undertaken.

(iii) Computational Studies. Density functional theory (DFT) analyses of electronic structure were carried out using the computationally efficient model systems $[CpFe(dmpe)(EX)]^+$ (EX = GaI, BF, CO, and N_2; dmpe = 1,2-bis(dimethylphosphino)ethane, $Me_2PCH_2CH_2PMe_2$), bonding analyses for which are discussed below. For all four ligands, essentially linear minimum energy geometries are obtained, with that for EX = GaI ($\angle$Fe−Ga−I = 174.4°) being consistent with the major component of the solid state structure. Moreover, in order to rationalize the soft librational deformation implied by crystallographic measurements, calculations were also carried out on the larger system $[Cp^*Fe\{Me(Ph)PCH_2CH_2P(Ph)MePh\}(GaI)]^+$, in which the phenyl groups proximal to the GaI ligand and the methyl groups of the Cp* ligand are retained, so as to provide more reliable modeling of the GaI ligand environment in **9**.[46] A very shallow potential energy surface is found for the Fe−Ga−I bending deformation (ΔE < +3.5 kJ mol^{-1} for 159 < ϑ < 179°). Consistent with this, a relatively small energy increase (+11 kJ mol^{-1}) is associated with a Fe−Ga−I angle (149°) analogous to that found for the "bent" conformer of **9** in the solid state (see the Supporting Information for details of the energy profile). This energy difference is comparable to binding energies typically associated with halogen···arene interactions (e.g., 12.6−20.9 kJ mol^{-1} for "complexes" between halogens and various substituted benzenes, as determined from charge transfer bands),[47] and the existence of such contacts in the solid state structure of **9** [signaled by distances from I′ to C(55)−C(58) (3.437−3.665 Å) which are within the sum of the respective van der Waals radii][9] then offers a rationale for the bent structure of the minor (21%) component found in the crystal.

From a bonding perspective, a breakdown of the covalent (orbital) components of the metal−ligand bonds of each of the four model compounds reveals notable similarities (see Table 2);[48] in each case, partitioning of the bonding density implies that orbital interactions of π symmetry represent a significant fraction of the covalent bond [i.e., 33 (GaI), 42 (BF), 39 (CO), and 38% (N_2) of the total covalent bonding density]. However, taken in isolation, such an analysis is somewhat misleading, since it merely compares the relative σ/π breakdowns for each complex, without quantifying the *absolute magnitude* of the orbital (and other) contributions to the metal−ligand bond. To enable a more in-depth comparison, the fragment correlation

(42) Uhl, W.; Benter, M.; Melle, S.; Saak, W.; Frenking, G.; Uddin, J. *Organometallics* **1999**, *18*, 3778.
(43) For other examples of complexes containing base-stabilized EX fragments as ligands, see, for example: (a) Fischer, R. A.; Schulte, M. M.; Weiss, J.; Zsolnai, L.; Jacobi, A.; Huttner, G.; Frenking, G.; Boehme, C.; Vyboishchikov, S. F. *J. Am. Chem. Soc.* **1998**, *120*, 1237.
(44) Power, P. P. *Chem. Rev.* **1999**, *99*, 3463.
(45) Melzer, D.; Weiss, E. *J. Organomet. Chem.* **1984**, *263*, 67.
(46) Analogous calculations on the "full" cation $[Cp^*Fe(dppe)(GaI)]^+$ at an acceptable level of theory did not satisfy all of the convergence criteria.
(47) Rosokha, S. V.; Kochi, J. K. *Struct. Bonding (Berlin)* **2007**, *126*, 137.
(48) Under the energy decomposition analysis employed, the interaction energy ΔE_{int} between two fragments is given by the sum of attractive orbital (ΔE_{orb}) and electrostatic ($\Delta E_{electrostat}$) and repulsive Pauli (ΔE_{Pauli}) terms.[6c] $\Delta E_{int} = \Delta E_{orb} + \Delta E_{electrostat} + \Delta E_{Pauli}$.

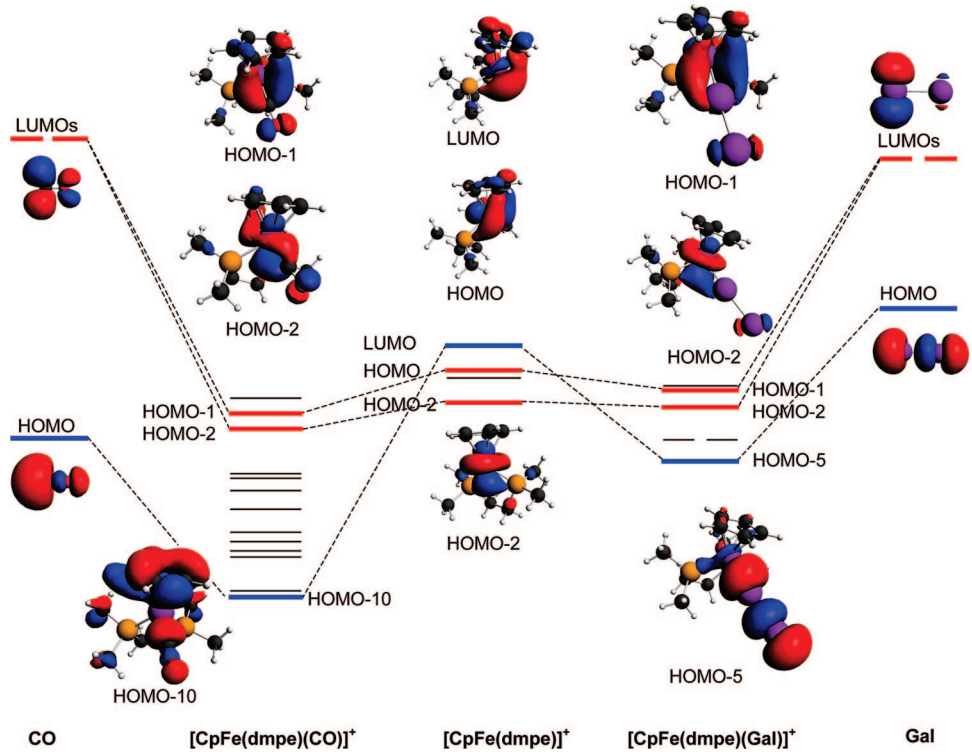

Figure 5. Molecular orbital energy level diagram for the model complexes $[CpFe(dmpe)(CO)]^+$ and $[CpFe(dmpe)(GaI)]^+$ showing correlation with the $[CpFe(dmpe)]^+$ and CO/GaI fragments. Local σ symmetry interactions involving the LUMO of $[CpFe(dmpe)]^+$ and the HOMO of the CO/GaI ligand are shown in blue; π symmetry interactions originating in the HOMO and HOMO-2 of $[CpFe(dmpe)]^+$ and the degenerate pair of LUMOs of CO/GaI are shown in red.

diagrams for $[CpFe(dmpe)(CO)]^+$ and $[CpFe(dmpe)(GaI)]^+$ were determined and are reproduced in Figure 5. The HOMOs for both compounds are dominated by a metal centered d-orbital with δ-symmetry along the Fe−C/Ga vector; this orbital is therefore nonbonding for the CO/GaI ligands. The HOMO/HOMO-2 and LUMO states for the $[CpFe(dmpe)]^+$ fragment present π- and σ-symmetry,[49] respectively, at the vacant coordination site, and so bonding between this fragment and CO/GaI has the potential to include both σ-donation from the ligand to the metal center and π-back-donation. The primary contribution to bonding in each case involves the states of σ-symmetry, with the CO ligand showing a much stronger interaction with the metal center than GaI. Indeed, for $[CpFe(dmpe)(CO)]^+$, a number of other molecular orbitals (involving interactions of the metal center with the phosphine and cyclopentadienyl ligands) are actually present at energies *higher* than that of the primary Fe−CO σ-bonding orbital. This orbital in the CO case is the HOMO-10 (at −11.72 eV), whereas the corresponding orbital for the GaI complex is the HOMO-5 (at −9.55 eV; Figure 6).

For each complex there are also two sets of orbitals which could conceivably be characterized by metal to CO/GaI π bonding; the two degenerate π^* antibonding orbitals of the ligand can interact with complementary metal d-orbitals, i.e. the mutually orthogonal HOMO and HOMO-2 of $[CpFe(dmpe)]^+$. The bonding MOs so formed are lower in energy for $[CpFe(dmpe)(CO)]^+$ (HOMO-1 and HOMO-2 at −8.44 and −8.83 eV, respectively) than for $[CpFe(dmpe)(GaI)]^+$ (−7.95 and −8.34 eV), despite the higher energy LUMO states for the CO ligand (−2.24 eV cf. −2.70 eV for GaI). Thus, as in the case of the σ bonding manifold, significantly smaller perturbations of the bonding MOs are observed for the π symmetry interactions of the GaI complex (cf. CO). As such, it seems likely that the relatively similar σ and π ratios calculated for the GaI and CO complexes (67:33 and 61:39, respectively; Table 2) are reflective of marked reductions in *both* the σ *and* π orbital interactions for the GaI ligand. This supposition is corroborated by explicit calculation of the orbital, electrostatic, and Pauli energetic contributions to the metal−ligand bond (*vide infra*).[48] Moreover, in terms of the π symmetry atomic orbitals at gallium, Figure 7 gives an idea of the MOs to which these ultimately contribute in the model complex $[CpFe(dmpe)(GaI)]^+$. Thus, the HOMO-3 and HOMO-1 orbitals [at −9.06 and −7.95 eV; Figure 7a and b], which feature in-phase combinations of Ga $4p_x$ with the I $5p_x$ and Fe $3d_{xy}$ orbitals, respectively, feature 4.3 and 6.2% contributions from the gallium orbital. By contrast, the antibonding LUMO+3 (−4.94 eV) features a 71.6% contribution from Ga $4p_x$, a finding which also points to the

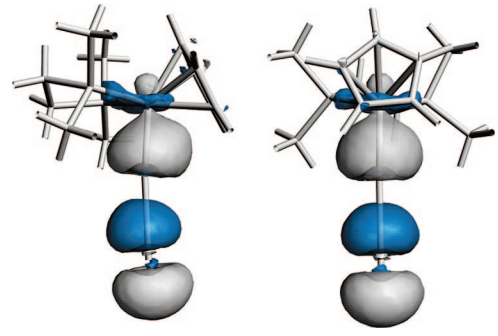

Figure 6. Orbital 41 (HOMO-5) for $[CpFe(dmpe)(GaI)]^+$: the metal ligand σ bonding MO.

(49) Schilling, B. E. R.; Hoffmann, R.; Lichtenberger, D. *J. Am. Chem. Soc.* **1979**, *101*, 585.

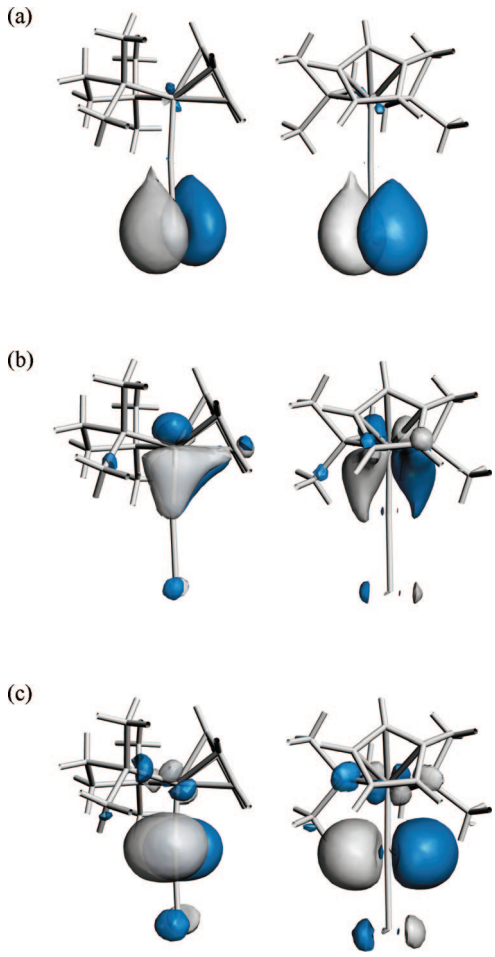

Figure 7. MOs for $[CpFe(dmpe)(GaI)]^+$ featuring contributions from the Ga $4p_x$ orbital: (a) the HOMO-3; (b) the HOMO-1; and (c) the LUMO+3.

relatively weakly bonding nature of any interactions in which this atomic orbital is involved.

In energetic terms, the magnitude of the covalent (orbital) bonding component for the GaI complex (-236 kJ mol^{-1}) can be put into context by values of -469, -397, and -262 kJ mol^{-1} for the corresponding BF, CO, and N_2 complexes and by a value of -234 kJ mol^{-1} for the *electrostatic* contribution to the (significantly polar) Fe−GaI bond. Presumably, despite the higher energy of the HOMO for GaI (-6.08 eV cf. -9.03 eV for CO, Figure 5) and the greater localization of the LUMO at the donor atom (plus its lower energy), the weaker orbital contribution for GaI reflects (at least in part) the more diffuse nature of the 4s/4p derived orbitals at gallium and less effective interaction with the fragment orbitals of $[CpFe(dmpe)]^+$.[49] Thus, overall metal−ligand interaction energies [$\Delta E_{int} = -103$ (GaI), -285 (BF), -213 (CO), and -120 kJ mol^{-1} (N_2)] reveal significantly weaker binding of the GaI ligand,[7–9] and corroborate its experimentally observed (quantitative) displacement from **9** by the addition of carbon monoxide to give $[Cp^*Fe(dppe)(CO)]^+[BAr^f_4]^-$.

Conclusions

Halide abstraction has been shown to be a viable method for the generation of mononuclear cationic complexes containing gallium donor ligands. The ability to isolate tractable two-coordinate products, however, is strongly dependent on the steric and electronics properties of the metal/ligand fragment. In the case of complexes containing ancillary π-acceptor ligands such as CO, cationic complexes can only be isolated as base-trapped adducts, even with bulky aryl substituents at gallium. *Base-free* gallylene species such as $[Cp^*Fe(CO)_2GaMes]^+$ can be identified only in the vapor phase by electrospray mass spectrometry experiments. With bis(phosphine) donor sets at the metal, the more favorable steric/electronic environment allows for the isolation of two-coordinate ligand systems, *even with halide substituents at gallium*. Thus, $[Cp^*Fe(dppe)(GaI)]^+[BAr^f_4]^-$ (**9**) can be synthesized and shown crystallographically to feature a terminally bound GaI ligand; **9** represents the first experimental realization of a complex containing a valence isoelectronic group 13/group 17 analogue of CO and N_2. DFT calculations reveal a relatively weakly bound GaI ligand, which is confirmed experimentally by the reaction of **9** with CO to give $[Cp^*Fe(dppe)(CO)]^+[BAr^f_4]^-$. In the absence of such reagents, **9** is stable for weeks in fluorobenzene solution, presumably reflecting (i) effective steric shielding of the gallium center by the ancillary phosphine and Cp* ligands; (ii) a net cationic charge which retards the tendency toward dimerization found for putative charge neutral systems; and (iii) (albeit relatively minor) population of the LUMOs of the GaI molecule through π overlap with the HOMO and HOMO-2 of the $[Cp^*Fe(dppe)]^+$ fragment.

Acknowledgment. We thank the EPSRC for funding, including the National Crystallography and Mass Spectrometry Services; STFC for access to synchrotron facilities; and A. S. Weller, A. Lubben, D. L. Kays, and C. Tang for assistance with mass spectrometry and other compound characterization.

Supporting Information Available: Crystallographic data for $[Cp^*Fe(CO)_2]_2GaN(SiMe_3)_2$ (**7**), $[\{Cp^*M(CO)_2\}_2(\mu\text{-I})]^+[BAr^f_4]^-$ (**10**, M = Fe; **17**, M = Ru), and $[Cp^*Fe(dppe)Cl]^+[BAr^f_4]^-$ (**11**); spectroscopic and crystallographic data for $[Cp^*Ru(CO)_2GaI_2]_2$ (**13**) and details of its reactivity toward dppe; spectroscopic and crystallographic data for $[Cp^*Ru(CO)_2GaI_2]_2(\mu\text{-dppe})$ (**14**) and Cp*Ru(dppe)I (**15**); and details of DFT calculations. This material is available free of charge via the Internet at http://pubs.acs.org.

JA806655F